Clay mineralogy, strontium and neodymium isotope ratios in the sediments of two High Arctic catchments (Svalbard)

Ruth S. Hindshaw[1], Nicholas J. Tosca[2], Alexander M. Piotrowski[1], and Edward T. Tipper[1]

[1]Department of Earth Sciences, University of Cambridge, Downing Street, Cambridge, UK, CB2 3EQ
[2]Department of Earth Sciences, University of Oxford, South Parks Road, Oxford, UK, OX1 3AN

Correspondence to: R. S. Hindshaw (ruth.hindshaw@gmail.com)

Abstract. The identification of sediment sources to the ocean is a pre-requisite to using marine sediment cores to extract information on past climate and ocean circulation. Sr and Nd isotopes are classical tools with which to trace source provenance. Despite considerable interest in the Arctic Ocean, the circum-Arctic source regions are poorly characterised in terms of their Sr and Nd isotopic compositions. In this study we present Sr and Nd isotope data from the Paleogene Central Basin sediments of Svalbard, including the first published data of stream suspended sediments from Svalbard.

The stream suspended sediments exhibit considerable isotopic variation (εNd = -20.6 to -13.4; ^{87}Sr/^{86}Sr = 0.73421 to 0.74704) which can be related to the depositional history of the sedimentary formations from which they are derived. In combination with analysis of the clay mineralogy of catchment rocks and sediments, we suggest that the Central Basin sedimentary rocks were derived from two sources. One source is Proterozoic sediments derived from Greenlandic basement rocks which are rich in illite and have high ^{87}Sr/^{86}Sr and low εNd values. The second source is Carboniferous to Jurassic sediments derived from Siberian basalts which are rich in smectite and have low ^{87}Sr/^{86}Sr and high εNd values. Due to a change in depositional conditions throughout the Paleogene (from deep-sea to continental) the relative proportions of these two sources varies in the Central Basin formations. The modern stream suspended sediment isotopic composition is then controlled by modern processes, in particular glaciation, which determines the present-day exposure of the formations and therefore the relative contribution of each formation to the stream suspended sediment load. This study demonstrates that the ~~Sr and~~ Nd isotopic composition of stream suspended sediments ~~from the continents~~ exhibits seasonal variation, which likely mirrors longer-term hydrological changes, with implications for source provenance studies based on fixed ~~sources~~ end-members through time.

1 Introduction

Since the Miocene, the Arctic has been subject to the repeated advance and retreat of ice sheets, a record of which is preserved in ocean sediments (Svendsen et al., 2004; Knies and Gaina, 2008). Thus, the Arctic Ocean and its surrounding seas are a key region for developing our understanding of past ice sheet dynamics and climate. A considerable number of ocean cores have been drilled in this region, allowing us to access the sedimentary archive (e.g. Vogt et al., 2001; Spielhagen et al., 2004; Knies and Gaina, 2008; Hillaire-Marcel et al., 2013; Fagel et al., 2014; Meinhardt et al., 2016). They provide information on past ocean chemistry through analysis of foraminifera (e.g. Knies et al., 2014), on iceberg abundance through analysis of ice-rafted

debris (IRD, e.g. Spielhagen et al., 2004) and on past sediment sources through analysis of the mineralogy and geochemistry of the sediment (e.g. Meinhardt et al., 2016).

Clay mineralogy in ocean sediment cores is often used to reconstruct paleoclimate and paleoceanography (e.g. Winkler et al., 2002). However, both the source rock and weathering conditions on the continents affect which clay minerals are formed. For example, kaolinite is more likely to form in tropical climates with intense chemical weathering, whereas illite is more likely to form where physical weathering dominates (Singer, 1984). The weathering of basalt will likely lead to the formation of smectite, whereas the weathering of granite will likely lead to the formation of illite or kaolinite (Essington, 2004). The Arctic Ocean has a wide variety of source regions (geographical regions with relatively homogenous lithology) ranging from Siberia (young basalts) to Greenland (Precambrian rocks) ~~young basalts in Siberia to the Precambrian rocks of Greenland~~ and it is therefore imperative for paleoclimate studies to identify which changes in clay mineralogy are related to a change in climate and which are related to a change in source region.

The radiogenic isotope tracers $^{143}Nd/^{144}Nd$ (expressed as εNd) and $^{87}Sr/^{86}Sr$ are often used together to understand where and how sediment is generated and weathered, enabling source regions to be characterised (Goldstein and Jacobsen, 1988; Cameron and Hattori, 1997; Tricca et al., 1999; Peucker-Ehrenbrink et al., 2010; Lupker et al., 2013; Clinger et al., 2016). εNd is particularly suited to being a source tracer because, unlike Sr and Rb which are fluid mobile, Sm and Nd are immobile and behave very similarly during chemical weathering such that the Sm/Nd ratio does not fractionate during weathering (McCulloch and Wasserburg, 1978) and therefore variations in εNd are predominantly controlled by age (Goldstein and Jacobsen, 1988) rather than the weathering of specific minerals which can affect the Rb-Sr system (e.g. Bullen et al., 1997).

Although weathering effects on the neodymium isotopic composition of sediments are considered essentially negligible, it has been shown that in certain circumstances preferential leaching of minerals with a different Sm/Nd ratio to bulk rock can lead to variations in εNd in soil profiles (Öhlander et al., 2000; Aubert et al., 2001), which could affect the εNd value of the derived sediments. Variations within soil profiles are either attributed to dust inputs (Viers and Wasserburg, 2004; Ma et al., 2010) and/or the dissolution of accessory phases such as phosphate minerals or Fe-Mn oxyhydroxides (Goldstein and Jacobsen, 1987; Öhlander et al., 2000; Aubert et al., 2001; Babechuk et al., 2015). Additionally, εNd variations in ocean sediments are often interpreted in terms of changing source regions with the isotopic composition of individual source regions remaining constant though time. However, recent studies have hinted at seasonal variations in εNd in river sediments (Viers et al., 2008; Garçon et al., 2013; Lupker et al., 2013), raising the possibility that the εNd value of sediment exported from individual source regions may not remain constant over time. Thus, although εNd is a reliable tracer of source, one region may contain multiple ~~sources~~ end-members, whose relative contributions vary over time.

The source regions to the Arctic Ocean are in general relatively poorly characterised in terms of coupled εNd and $^{87}Sr/^{86}Sr$ measurements with only a few samples from the major rivers and shelf sediments (Eisenhauer et al., 1999; Hillaire-Marcel et al., 2013). Svalbard (Fig. 1) is particularly important to characterise owing to its location by the Fram Strait, which is the site of deep water formation essential to the functioning of the global thermohaline circulation, and has therefore been the target of studies seeking to understand the formation of the Atlantic-Arctic gateway (Jakobsson et al., 2007). However, there is neither $^{87}Sr/^{86}Sr$ nor εNd data on river sediments from Svalbard. Previous studies (Tütken et al., 2002; Maccali et al., 2013)

have taken the bedrock data of granitoids from Ny Friesland in the north-east of Spitsbergen (the largest island in the Svalbard archipelago, Fig. 2, Johansson et al., 1995; Johansson and Gee, 1999) to represent the Svalbard source region. Svalbard has a wide range of rocks from different ages and in this study we characterise sediments from two catchments located in the Paleogene Central Basin, which comprises 8% of the land area of Svalbard, and from which no prior Sr-Nd measurements exist. Being relatively sparsely glaciated and more easily eroded, these sedimentary formations could constitute an important sediment source from Svalbard. The studied catchments have nominally identical lithology but one is glaciated, allowing us to examine the effect of glaciation on stream suspended sediment composition. As clay minerals are the main constituent of the rocks in the study area, we combine the geochemical data (εNd and ^{87}Sr/^{86}Sr) with clay mineralogy in order to identify the factors influencing the unexpectedly large variation in radiogenic isotope compositions observed in the catchment sediments.

2 Field site

Svalbard is located in the Arctic Ocean (Fig. 1) and has an Arctic climate. In 2012 (the year samples were collected) the mean temperature was -2.0 °C and precipitation was 268 mm, as recorded at Longyearbyen Airport (Nordli et al., 2012). Permafrost is continuous throughout the islands (Humlum et al., 2003). Two catchments were studied which are situated adjacent to each other approximately 5 km south of Longyearbyen in central Svalbard (Fig. 2a).

The first catchment is a permafrost-affected valley called Fardalen (Fig. 2c) which is likely to have been unglaciated for at least the last 10 kyr (Svendsen and Mangerud, 1997). The catchment area is 3.4 km^2 and ranges in elevation from 250 - 1025 m.a.s.l. The second catchment contains a glacier called Dryadbreen and 'Dryadbreen' will be used hereafter to refer to the whole catchment and not just the glacier. Between 1936 and 2006 the area of the glacier decreased from 2.59 to 0.91 km^2 leaving large terminal and lateral ice-cored moraines and a sandur in front of the glacier (Ziaja and Pipała, 2007). The catchment area is 4.8 km^2 and ranges in elevation from 250 - 1031 m.a.s.l.

2.1 Geological background

The two studied catchments are situated in the Paleogene sedimentary Central Basin of Svalbard (Fig. 2a). The sedimentary formations exposed in the catchments are from the Van Mijenfjorden group which is Paleocene to Eocene in age (66 - 33.9 Ma) and contains sandstones, siltstones and shale (Fig. 2b, Major et al., 2000). The formations exposed in the two catchments have been relatively well studied on account of the fact they cover the Paleocene-Eocene Thermal Maximum (PETM) and formed as a consequence of sedimentation which commenced upon the separation of Greenland from Eurasia (e.g. Helland-Hansen, 1990; Müller and Spielhagen, 1990; Cui et al., 2011; Dypvik et al., 2011; Elling et al., 2016; Jones et al., 2016).

The Central Basin sediments are divided into six formations (Major et al., 2000) which were deposited in a series of transgressive-regressive cycles. The youngest four are exposed in the studied catchments. It is thought that the source for the oldest sediments (mid-Paleocene to early Eocene) was from the east (Carboniferous to Jurassic Siberian basalts, Helland-Hansen, 1990), but this changed to the west (Proterozoic Greenlandic/Canadian High Arctic Shield) during early to mid-Eocene

with the erosion of the uplifted West Spitsbergen Fold and Thrust Belt whose formation is linked to rifting of the North Atlantic and the separation of Svalbard from Greenland.

The oldest formation exposed in the studied catchments is the Grumantbyen Formation (Fig. 2b), comprising shallow marine sandstones. The Grumantbyen sediments are part of a regressive trend with sediment derived from the east and possibly the north (Helland-Hansen, 1990). The youngest three formations comprise a regressive sequence with (from oldest to youngest) the Frysjaodden formation comprising fine-grained shales deposited offshore in an open basin; Battfjellet Formation comprising shallow marine sandstone; and Aspelintoppen comprising continental deposits (Helland-Hansen, 1990; Müller and Spielhagen, 1990). The mountain belt is thought to have eroded rapidly (Cui et al., 2011) based on the immaturity of the sandstones (Helland-Hansen, 1990). Detection of pre-Caledonian metamorphic detritus indicates that the mountain belt was eroded down into the basement rocks (Helland-Hansen, 1990). The PETM boundary is near the base of the Frysjaodden Formation (Charles et al., 2011).

3 Methods

A selection of 18 representative solid samples, including sedimentary rocks, bedload sediments and glacial sediment, were sampled from both catchments. The sedimentary rock samples were first crushed (jaw crusher) and were subsequently ground to fine powders (rotary disc mill and planetary ball mill). For the sediment samples, only the latter step was required. A subset of samples (Fig. 2c) were selected for element and isotopic analysis (Table 1) and they are further described here. For all other samples a brief description is included in Table 2. Samples 'G' and 'R01' are two separate samples of frost-shattered angular pieces of shale, 1 - 4 cm in length collected from the Frysjaodden Formation in the unglaciated Fardalen catchment. Samples 'R02' (frost-shattered wacke), 'R03' (litharenite), 'R04' (shale) and 'D' (coarse sediment from glacier surface) were collected from the glaciated Dryadbreen catchment where transport and physical erosion by the glacier has combined rocks from different formations. Additionally, sediment from the stream channels of each catchment were collected (samples 'L' and 'O'). Stream suspended sediment ($>0.2\ \mu$m) was retrieved from nylon filter papers during water sample collection (Hindshaw et al., 2016) by washing the filter paper with deionized water and then freeze drying the sample. Stream suspended sediment samples were collected from each of the catchment streams on alternate days during June (snow melt) and July/August (summer) 2012, just before their confluence with the main valley stream (Fig. 2c). Part of each sample was treated with 5% HCl to remove carbonates. The leachates were not retained. A subset of four samples, one from each season and each catchment were analysed for this study (Table 1). Discharge measurements are only available for summer; the discharge at the time of sample collection for the two summer samples was 0.24 m s^{-1} (Fardalen) and 0.35 m s^{-1} (Dryadbreen) (Hindshaw et al., 2016). Suspended sediment concentrations at the time of sampling are reported in Table 1.

3.1 Semi-quantitative determination of clay mineral abundances

A $<2\ \mu$m size-fraction was separated from bulk sediment by repeatedly rinsing and re-suspending the sample in de-ionized water with sodium phosphate as a dispersal agent, followed by sonication. The $<2\ \mu$m fraction was separated by centrifugation

(Moore and Reynolds Jr., 1997) and was then transferred to a clean glass slide in preparation for XRD using a filter-peel technique to orientate the sample (Moore and Reynolds Jr., 1997). XRD analysis was performed on a PANalytical PW1050 X-ray diffractometer with a Hiltonbrooks DG2 X-ray generator (Co-Kα radiation) at the University of St. Andrews. Data were collected between 5 and 40° with a step size of 0.02° and a counting time of 3 s per step. Spectra were collected on air-dried, glycerol-treated, 450°C heated and 550°C heated samples. The glycerol-treated and 450°C spectra were used to obtain semi-quantitative clay mineral abundances using the method outlined in Griffin (1971) which uses the peak heights of kaolinite 001 and illite 001 in the 450°C spectrum and the peak heights of chlorite 004, kaolinite 002, kaolinite 001 and illite 001 in the glycerol treated spectrum to give the relative abundances of kaolinite, chlorite, illite (mica) and expandable layer clay minerals (e.g. smectite and mixed-layer minerals containing smectite).

3.2 Chemical and isotopic composition

A selection of bulk solid samples and separated clay fractions were analysed for major and trace element chemistry using the following method: approximately 100 mg of material was ashed at 950°C for 120 minutes. The sample was then digested in a mixture of concentrated hydrofluoric and nitric acids and repeatedly dried down and re-dissolved in 6M HCl. In the final step, the dried down sample was re-dissolved in 2% HNO_3. Major and trace element concentrations were measured at the University of Cambridge by inductively-coupled plasma optical emission spectrometry (ICP-OES, Agilent Technologies 5100) and quadrupole inductively-coupled plasma mass spectrometry (Q-ICP-MS, Perkin Elmer 63 Nexion 350D), respectively. Si concentrations were calculated by difference assuming 100% recovery. The accuracy of the Si concentrations obtained in this way was confirmed by comparison with XRF obtained for four samples (Table A1). The accuracy of the concentration measurements was verified by repeated measurements of seven different USGS rock standards (Tables A3 and A4), including two shale standards (SCo-1 and SGR-1b). The procedural blanks through the digestion procedure were negligible (<0.1% sample) for Sr and Nd.

Neodymium was separated from the matrix using the method described in Piotrowski et al. (2009). This method uses two columns. The first column contained Eichrom TRUspec resin which separates out REE from the matrix and the second column contains Eichrom LNSpec resin to isolate Nd. The radiogenic neodymium isotopic composition was measured on a Nu plasma (Nu Instruments, University of Cambridge) multi-collector inductively coupled plasma mass spectrometer (MC-ICP-MS). Samples were run at 50-75 ppb with an APEX ACM sample introduction system. Samples were run in triplicate (three measurements on different days) with each measurement comprising 30 cycles with 10 s integration. Samarium interferences were monitored by measuring mass 149. No interferences were detected and oxides were monitored during tuning to ensure they were well below 0.5% of the beam size. The exponential law was applied to correct for instrument mass fractionation and all $^{143}Nd/^{144}Nd$ ratios were normalised to $^{146}Nd/^{144}Nd$ = 0.7219. Standard-sample ~~were~~ bracketing was employed in order to correct for the offset with the accepted JNdi-1 value: 0.512060±0.000024 (2SD, n=119) compared with the accepted value of 0.512115 (Tanaka et al., 2000). The USGS shale standard SCo-1 was measured and the $^{143}Nd/^{144}Nd$ value of 0.512086±0.000029 (n=3, 2SD) is in agreement with a previously published value of 0.512117±0.000010 (2σ, n=20

Krogstad et al., 2004). Neodymium isotope ratios are reported as deviations relative to the chondritic uniform reservoir (CHUR, ^{143}Nd/^{144}Nd = 0.512638, Jacobsen and Wasserburg, 1980).

Strontium was separated from the matrix using Biorad mirco bio-spin columns with Eichrom SrSpec resin (Hindshaw, 2011). The radiogenic strontium isotopic compositions were measured on a Neptune MC-ICP-MS (Thermo, University of Cambridge) and were run at 50 ppb using an APEX sample introduction system. Samples were run in triplicate (three measurements on different days) with each measurement comprising 30 cycles with 8 s integration. ^{85}Rb was monitored to correct for rubidium interferences on ^{87}Sr and data were additionally corrected for Kr interferences by measuring ^{83}Kr. The exponential law was applied to correct for instrument mass fractionation and all ^{87}Sr/^{86}Sr ratios were normalised to ^{86}Sr/^{88}Sr = 0.1194. Measurements of NBS 987 gave a ^{87}Sr/^{86}Sr value of 0.710249±29 (2SD, n=27) and the seawater value was 0.709188±24 (2SD, n=9), which is within error of the accepted value of 0.709179±8 (2σ, n=17 Mokadem et al., 2015).

4   Results

The major and trace element concentrations of the solid samples are provided in Table 1. The measured values are typical for shales (Taylor and McLennan, 1985) and the rare earth element (REE) chondrite normalised element profile of these samples closely follows that of the Post Archaean Australian Shale (PAAS, Table A2). Strontium and neodymium concentrations varied from 78 to 139 and 25 to 49 ppm, respectively. The two rock samples collected from the Frysjaodden Formation (R01 and G) have very similar major element compositions to core samples from this formation (Fig. 3, Schlegel et al., 2013). The formations in the glaciated catchment were not clearly exposed due to the presence of moraine material. However, the core sample from the Asplintoppen Formation is classified as a litharenite (Fig. 4) and as sample R03 is a litharenite and has similar major element chemistry (Fig. 3), we infer that this sample is also derived from the Aspelintoppen Formation. Sample R02 plots close to the wacke-shale boundary in Fig. 4 and in terms of major element chemistry it plots on the edge of the area defined by the Frysjaodden samples (Fig. 3). We therefore infer that this sample originated close to the boundary between the Frysjaodden and Battfjellet formations. Sample R04 is classified as a shale (Fig. 4) but its major element composition is distinct from the Frysjaodden Formation samples, in particular for Fe_2O_3 (Fig. 3). Given that this sample was collected on the surface of the glacier, it is likely that it is a shale derived from either the Battfjellet or Aspelintoppen Formation. These assignments are corroborated by the clay mineralogy (see below).

There ~~was~~ is a large range in both the strontium and neodymium isotopic compositions of the bulk solid samples: ^{87}Sr/^{86}Sr = 0.72449 to 0.75243 and εNd = -24.2 to -11.9 (Table 1). Radiogenic Sr and Nd values are inversely correlated (Fig. 5) and in general, samples collected from the unglaciated Fardalen catchment e.g. R01 and G have higher ^{87}Sr/^{86}Sr and lower εNd values than those samples collected in the glaciated Dryadbreen catchment e.g. D and O (Table 1).

The clay-sized fraction forms a parallel array to the bulk rock samples in εNd-^{87}Sr/^{86}Sr space (Fig. 5), with the clay-sized samples having higher εNd and lower ^{87}Sr/^{86}Sr values (except for R01). The εNd values of clay fractions were 2.1 to 3.2 epsilon units higher than the corresponding bulk sample and ^{87}Sr/^{86}Sr values were 1030 to 2030 ppm lower in the clay compared to the bulk, apart from sample R01 where the clay was 1100 ppm higher in the clay than in the bulk. Rubidium,

strontium, neodymium and samarium concentrations in clay samples are comparable to, or higher than, bulk values (Table 1). Given that clay minerals constitute >88% of the non-quartz minerals in these samples (Hindshaw et al., 2016), clays are the main host of these elements. In a compilation of river sediments from all over the world, the clay fraction εNd value was observed to be greater than the silt-sized fraction by an average of 0.8 epsilon units (Bayon et al., 2015). ~~It has been~~
5 ~~observed that in a compilation of river sediments from all over the world that εNd in the clay fraction is greater than in the silt-sized fraction by an average of 0.8 epsilon units (Bayon et al., 2015).~~ Fine sediments (as measured by Al/Si ratio) from the Mackenzie River have also been observed to have higher values than coarser sediments (Vonk et al., 2015). The offset in εNd between fine and coarse fractions has been interpreted to reflect the preferential transport of basalt and volcanics in the fine fraction (McLennan et al., 1989; Garçon and Chauvel, 2014; Bayon et al., 2015). A volcanic signal is typically only
10 observed in the first sedimentary cycle, due to the rapid chemical weathering of volcanic particles (McLennan et al., 1989) and therefore, if volcanics are present, they must have been deposited at the same time as the Central Basin sediments. Potential volcanic sources for this period could be the volcanic provinces of North Greenland and Ellesmere Island (58-61 Ma, Jones et al., 2016).

The residues of suspended sediments (collected on 0.2 μm filter paper) after treatment with 5% HCl had higher ^{87}Sr/^{86}Sr
15 (3528-4832 ppm) and lower εNd values (1.0 to 4.6 epsilon units) than the corresponding unleached sediment.

4.1 Semi-quantitative clay abundance

Illite, chlorite and kaolinite were present in all the samples analysed. In addition, the presence of an expandable layer clay mineral is also evident in the collapse of the XRD signal around 12.7 Å (8 °2θ Co radiation) between the air-dried and glycerol-treated spectra (Fig 6). Additionally, the asymmetry of the illite 001 peak (Fig. 6) suggests that this expandable
20 layer clay mineral is an illite-smectite mixed-layer phase (Moore and Reynolds Jr., 1997) and this is in agreement with the interpretation by Dypvik et al. (2011) of XRD spectra from core samples from the same formations exposed in the studied catchments. This mixed layer expandable phase will be referred to as 'I/S' in the following discussion. The relative proportions of illite, chlorite, kaolinite and I/S are given in Table 2.

The solid samples collected from the glaciated Dryadbreen catchment tend to have higher illite abundances and lower I/S
25 abundances than those samples collected from the unglaciated Fardalen catchment (Table 2). For all samples, there is an inverse relationship between the relative abundances of I/S and illite (Fig. 7b). The relative abundances of kaolinite and chlorite were similar in both catchments (Table 2). We are not able to distinguish between authigenic and detrital clay minerals.

The clay-sized fraction of the sedimentary rock samples from the Frysjaodden Formation (R01, G) have a lower relative proportion of illite than the samples inferred to be derived from the Battfjellet (R02) and Aspelintoppen (R03) formations (Fig.
30 7). This is in agreement with the decrease in the relative proportion of illite observed in the clay-sized fraction of core samples from the Aspelintoppen Formation (64%) to the Frysjaodden Formation (51%) (Schlegel et al., 2013). Samples with a high relative proportion of illite had high ^{87}Sr/^{86}Sr and low εNd values compared to those with a low relative proportion (Fig. 7c,d).

5 Discussion

The variation in clay mineralogy, ^{87}Sr/^{86}Sr and εNd could be caused by three scenarios: mixing between two or more sediment sources, sedimentary processes (either modern or in the Eocene), or a combination of source and process effects.

5.1 Sediment sources

5   The linear trend between ^{87}Sr/^{86}Sr and εNd is suggestive both of a common regional process affecting both isotope systems (Goldstein and Jacobsen, 1988) and of mixing between two end-members. The sediments deposited in the Central Basin during the Eocene were themselves derived from Mesozoic sediments. Based on zircon dating, it is thought that during the Mesozoic, the sediment source to Svalbard alternated between an older (Proterozoic) western component comprised of re-worked sediments from Greenland and Canada and a younger (Carboniferous-Jurassic) eastern component from Siberian fold-

10   and-thrust belts (Fig. 1, Bue and Andresen, 2014; Elling et al., 2016; Petersen et al., 2016). The erosion of the Siberian Traps which formed within the same time period (Permian to Triassic) would also have contributed sediment to the ocean. We will refer to these two sources as 'East' and 'West'.

The eastern source (Fig. 1, Lightfoot et al., 1993; Wooden et al., 1993; Spadea and D'Antonio, 2006) is relatively well-defined since the samples are essentially mono-lithologic (basaltic) and were deposited over a relatively short time-period.

15   Based on zircon dating, both the Uralides and the Verkhoyansk Fold-and-Thrust Belt (Fig. 1) have been identified as potential sources to Svalbard Mesozoic sediments and the Paleocene Basilika and Firkanten formations (Fig. 2b, both underlie the Grumantbyen Formation) (Bue and Andresen, 2014; Elling et al., 2016; Petersen et al., 2016). The western end-member is much harder to characterise as it consists of Precambrian rocks which have undergone extensive metamorphism. An end-member with εNd values lower than -23.3 is required (D, Table 1) and therefore only data from western Greenland is considered

20   (Fig. 1). The East coast was affected by the Caledonian orogeny (Henriksen, 1999) and later by the rifting of the North Atlantic (Bernstein et al., 1998) and therefore has higher (younger) εNd values (Jeandel et al., 2007). The range in ^{87}Sr/^{86}Sr and εNd from literature data of Archaean rocks from western and northern Greenland (Jacobsen, 1988; Collerson et al., 1989; Weis et al., 1997; Kalsbeek and Frei, 2006; Friend et al., 2009) is 0.70153 to 2.33356 and -56 to -2.75. By changing the Sr/Nd mass ratio of these two end-members, mixing lines can be drawn which encompass all the data, with the majority of points falling

25   on a mixing line with an r value of 1 (i.e. the Sr/Nd mass ratio of both end-members is the same, Fig. 8). The variation of ^{87}Sr/^{86}Sr and εNd in the clay-sized fraction forms a parallel trend to the bulk samples and can be explained by the same two end-members, but with a lower r value (Fig. 8). Variation in the r value between the bulk and the clay-sized fraction is to be expected given their different mineralogical compositions.

The variation in clay mineralogy (Fig. 7) can be explained by the different lithological sources of the two end-members (Fig.

30   8). Basalt typically weathers to smectite group minerals (e.g. Curtin and Smillie, 1981; Parra et al., 1985) and modern sediments originating from Siberia (basaltic) are enriched in smectite (Nürnberg et al., 1994; Wahsner et al., 1999). Any volcanic particles present will also tend to weather to smectite (Bayon et al., 2015). The western source is dominated by granitic rocks where the mica and K-feldspar typically weather to illite and kaolinite, respectively (Essington, 2004). Illite has high Rb/Sr ratios

and detrital illite is resistant to weathering, as the western source is older, this results in high ^{87}Sr/^{86}Sr and low εNd values. By contrast the younger eastern source will have lower ^{87}Sr/^{86}Sr and higher εNd values (Fig. 10). The lower ^{87}Sr/^{86}Sr and higher εNd values of the sedimentary rocks from the Frysjaodden Formation (G, R01) compared to those of the Battfjellet Formation (R04, Table 1) implies that the Frysjaodden Formation contains a greater proportion of the eastern end-member (Fig. 8). Indeed, zircon dating of samples from the Battfjellet Formation was consistent with a western, Greenland/Canadian Shield source, with an almost complete lack of Uralide aged grains (Petersen et al., 2016). The distinct differences between the two sources leads to the observed correlations between clay mineralogy, ^{87}Sr/^{86}Sr and εNd values (Figs. 7 and 10).

Mixing of two sediment sources can explain the difference between the stream suspended sediments collected in the two catchments (Fig. 5). Stream suspended sediments from the glaciated Dryadbreen catchment have lower εNd, higher ^{87}Sr/^{86}Sr values and a greater relative proportion of illite, compared to those from the unglaciated Fardalen catchment. These observations can be readily accounted for if the stream suspended sediments from Fardalen receive a greater relative contribution from the Frysjaodden Formation (enriched in the eastern end-member) than stream suspended sediments from Dryadbreen (Figs. 2 and 10). The lower relative contribution of the Frysjaodden Formation to stream suspended sediments from the glaciated Dryadbreen catchment can be explained by the moraine material being predominantly derived from sedimentary rocks once located in the upper reaches of the catchment (Aspelintoppen Formation), and the modern day sandur plain, containing the products of this physical erosion, essentially burying the lower ~~down~~ Frysajodden Formation. Changes in erosion caused by glaciation, which conveys sediment from the head to the toe of the glacier, could therefore influence the Sr and Nd isotopic of sediments exported to the ocean (von Blanckenburg and Nägler, 2001).

5.2 Sedimentary processes

5.2.1 Grain-size sorting

Sediments are sorted as a function of particle size as they travel through the water, such that coarser particles (typically primary minerals such as feldspar and quartz) will settle faster than finer particles (clay minerals). A size-sorting effect is observed in the difference between the ^{87}Sr/^{86}Sr and εNd values of the bulk and the clay-sized (<2 μm) fraction. This effect is observed at a global scale and is interpreted to reflect the preferential transport of volcanics and basalt in the fine fraction (Bayon et al., 2015). However, mineral sorting between a clay-sized fraction and a coarser fraction cannot account for the overall trend in the bulk samples (Fig. 5) as the clay minerals plot on a parallel array to the bulk samples (Fig. 5) indicating that the clay-sized fraction is not an end-member of the bulk sample trend. The offset between the clay-sized fraction and bulk is consistent with the clay-sized fraction being enriched in authigenic phases with higher εNd and lower ^{87}Sr/^{86}Sr compared to the bulk which is more likely to contain detrital minerals with a larger grain size.

Grain-size sorting could occur within the clay-sized fraction as illite will settle faster than smectite in the marine environment (Sionneau et al., 2008). The Frysjaodden Formation, being furthest away from shore, could become enriched in smectite-enriched particles derived from the basaltic eastern end-member whereas the Aspelintoppen Formation, deposited in a near-shore environment, could become enriched in relatively coarser illite-enriched particles derived from the granitic western

end-member. As clays form >88% of the non-quartz mineral fraction of the bulk (excluding R03 which does not plot on the main trend, Fig. 5, Hindshaw et al., 2016)), the trends observed between illite, smectite (I/S) and the radiogenic isotope compositions (Fig. 7) should be reflected in the bulk samples (Fig. 5).

5.2.2 Preferential leaching of a labile phase

5 There are examples from previous studies where chemical weathering has been identified as the cause of an inverse correlation between the relative proportions of illite and smectite (Fig. 7b, e.g. Setti et al., 2004). However, whilst modern day weathering processes can induce large variations in ^{87}Sr/^{86}Sr primarily as a result of large inter-mineral variations in the Rb/Sr ratio (e.g. Bullen et al., 1997), it is much harder to induce large variations in the Sm/Nd ratio of minerals and this ratio is often assumed to remain constant once a rock has been formed (e.g. McCulloch and Wasserburg, 1978). Preferential release of minerals with

10 different Sm/Nd ratios during chemical weathering has been implicated in the generation of small εNd offsets of around 2 epsilon units (Rickli et al., 2013) and larger variations in εNd were observed in a soil profile developed on granitic till in northern Sweden (Öhlander et al., 2000). In the latter study, a 7.7 epsilon unit variation was observed between the E horizon and the humic horizon, which was attributed to the preferential weathering of minerals enriched in Nd over Sm e.g. allanite.

In these catchments there is essentially no soil development due to recent glaciation and at the bulk scale the mineralogy

15 of the rocks is broadly similar (Hindshaw et al., 2016) as are their Sm/Nd ratios (Table 1). Additionally, the major element chemistry is very similar to that observed in core samples drilled through the same formations (Fig. 3, Schlegel et al., 2013), confirming that weathering processes since the Paleocene have had minor impact on bulk element and, by inference, ^{87}Sr/^{86}Sr and εNd values. The geochemical changes observed between formations in the core samples (Schlegel et al., 2013) were attributed to increased chemical weathering during the late Paleocene. In the given time period of this study (50 Ma) preferential

20 weathering of minerals with Sm/Nd ratios significantly different from bulk would be required in order to generate the 14 epsilon unit variation in εNd. In order to test this hypothesis, we applied a 5% HCl leach to remove easily leached mineral phases.

The chemical and isotopic composition of leached suspended sediment is distinct from bulk suspended sediment (Fig. 9a). From mass balance constraints, this points to the existence of a labile pool containing Ca, P, Mn and Fe, with low ^{87}Sr/^{86}Sr and high εNd (Table 1, Fig. 9a). Over 50% Ca is leached from the sediments with a Sr/Ca mass ratio of 0.002 to 0.007, consistent

25 with carbonate (Veizer, 1983), which would be expected to dissolve readily in 5% HCl (Tessier et al., 1979). A loss of P is also observed (39-56%, Table 1) suggesting the dissolution of apatite (containing Ca and Sr), and the decrease in Fe and Mn concentrations (Table 1) could be indicative of leaching Fe-Mn oxyhydroxides. In addition to apatite and carbonate, Sr could be derived from exchange sites within the clay minerals or adsorbed onto Fe-Mn oxyhydroxide surfaces. Further, the leaching procedure applied in this study is relatively aggressive and could have dissolved part of the clay mineral structure (Chester and

30 Hughes, 1967).

REE (rare earth element) patterns in leachates are commonly used to identify which mineral phases have been leached (e.g. Haley et al., 2004). The residual phase is depleted in MREE (middle REE) (Fig. 9b), implying the leachate is MREE enriched. A MREE enrichment is consistent with diagenetic apatite and Fe/Mn oxyhydroxides (Ohr et al., 1994; Tricca et al., 1999; Johannesson and Zhou, 1999; Su et al., 2017) and inconsistent with a carbonate phase, which is typically HREE enriched

(Byrne and Kim, 1990; Millero, 1992; Byrne and Sholkovitz, 1996), suggesting that Nd in the leachate is derived from the former phases. Volcanic ash also has a MREE enriched REE pattern (Tepe and Bau, 2014) and would have high εNd and low ^{87}Sr/^{86}Sr. However, the amount of a volcanic component is expected to be minor in the studied sediments as the volcanic ash component of particulates readily leaches upon contact with seawater (Pearce et al., 2013; Wilson et al., 2013) and therefore

5 may already have been leached during deposition in the Paleocene-Eocene. Additionally, volcanic ash in these layers has been diagenetically altered to bentonites (Cui et al., 2011; Elling et al., 2016; Jones et al., 2016) which are unlikely to be readily leached.

The shales in the Frysjaodden Formation were deposited in the marine environment and any authigenic minerals which were formed at that time are likely to have incorporated fluids with the Eocene seawater composition and deep-sea clays

10 are most susceptible to incorporating seawater (Dasch, 1969). Furthermore, smectite is the only clay mineral which forms in significant amounts in seawater (Griffin et al., 1968) and therefore it is very likely that the deep-sea Frysjaodden Formation contains authigenic smectite in addition to smectite derived from continental weathering, increasing the relative proportion of smectite in this Formation. In addition to diagenetic changes, adsorption may also occur. Samples containing a greater relative proportion of I/S, have a greater cation exchange capacity and are therefore more likely to contain a greater proportion of ions

15 from seawater, increasing the difference between ^{87}Sr/^{86}Sr and εNd in the residue and bulk (Dasch, 1969; Ohr et al., 1991). Adsorption of Nd from seawater was also implicated in a study by von Blanckenburg and Nägler (2001) where leachates of marine sediments had higher εNd than bulk and terrestrial sediments which had had no contact with seawater showed the reverse pattern (lower εNd in leachate compared to bulk). The greater difference between εNd in bulk and residue in the Fardalen (unglaciated) stream suspended sediments compared to Dryadbreen (glaciated, Fig. 9b) is therefore consistent with

20 the greater relative proportion of the Frysjaodden Formation to the Fardalen stream suspended sediments.

Assuming the leached phase is comprised of a mixture of authigenic minerals such as apatite and cations readily leached from clay minerals, then the leachate should have a seawater isotopic composition. Radiogenic Sr in seawater in the past is relatively well constrained given that it has a uniform value across the worlds oceans. Radiogenic neodymium, on the other hand, varies between ocean basins. A study based on fish, provides some constraints on the εNd and ^{87}Sr/^{86}Sr isotopic composition of the

25 Arctic Ocean during the Eocene (Fig. 1, Gleason et al., 2009), with ^{87}Sr/^{86}Sr varying from 0.7078 to 0.7088 and εNd varying from -7.5 to -5.5. If we assume that the location of this study and the area of the future Central Basin were connected, then this end-member would be within error of the eastern end-member and therefore could not be distinguished (Fig. 8). This is the most likely reason why the two trends (residue-bulk-leachate and east-west bulk) appear to fall on a common mixing line (Fig. 9a). Awwiller (1994) concluded that provenance information based on Nd-Sr isotopes could be obscured by the partial

30 incorporation of Sr and Nd from seawater. Diagenetic alteration has been implicated in shales which give unrealistically old Nd model ages (Arndt and Goldstein, 1987; Awwiller and Mack, 1991; Bock et al., 1994; Cullers et al., 1997; Krogstad et al., 2004). However, although the leached phase is isotopically distinct from bulk it cannot account for the isotopic difference observed between the residual phase isotopic compositions (Fig. 9a). Further, although the potential for diagenetic processes to modify bulk εNd and ^{87}Sr/^{86}Sr values cannot be ruled out, it is a subordinate effect to the primary trend of mixing between

35 distinct lithological end-members (Fig. 8).

5.3 Implications for Nd as a sediment source tracer

The stream suspended sediments observed in this study have highly heterogeneous Nd isotopic compositions with a difference between the two catchments of up to 6.8 epsilon units. Additionally, seasonal variation is observed in the unglaciated Fardalen catchment (1.6±0.4 epsilon units), but is not resolved in the glaciated Dryadbreen catchment (0.6±0.5 epsilon units). A similar magnitude of seasonal variation in εNd has previously been reported in the suspended sediments of much larger rivers. A 1.3 seasonal variation has been reported in suspended sediments from the Madeira River (Amazon, Viers et al., 2008) and a 2 epsilon unit range was observed in suspended sediments from two tributaries of the Ganges (Kosi and Narayani, Garçon et al., 2013). The seasonal variation in both of these studies was attributed to the seasonal variation in hydrology which affects how efficient the mixing of tributaries draining different geological units is. The role of hydrology and geology was recently demonstrated at a Canadian glacier where seasonal variations in εNd in a geologically heterogeneous catchment were attributed to the changes in subglacial hydrology (distributed to channelised) which altered where erosion occurred (Clinger et al., 2016). In contrast, glacial catchments with more homogenous lithology have little seasonal variation in εNd (Clinger et al., 2016; Rickli et al., 2017). From this small dataset (this study, Viers et al., 2008; Garçon et al., 2013; Clinger et al., 2016) it would appear that seasonal variations of εNd in suspended sediments are present where rivers drain mixed geology and have a pronounced seasonality to their hydrological cycle.

For the purposes of using Nd in ocean sediment cores as a tracer for past sediment sources it is assumed that the Nd isotopic composition of sediments is constant for broad ~~source~~ geographic regions (e.g. Jeandel et al., 2007), and this will not be affected by seasonal variations. However, seasonal cycles give an insight into weathering and erosion conditions under different hydrological regimes that are an analogue for longer term trends. It is entirely plausible that an intensified or weakened hydrological cycle could change the Nd isotopic composition of sediment export for a given region (Burton and Vance, 2000). Of particular relevance to the Arctic region is the re-organisation of drainage basins as the ice sheets waxed and waned and the attendant changes in magnitude and location of discharge to the ocean (e.g. Teller, 1990; Wickert, 2016). Therefore, it should not necessarily be assumed that the continental regions have had a constant εNd export to the oceans over glacial-interglacial timescales. For example, the 5.7 epsilon unit range in εNd (which is of similar magnitude to difference between catchments observed in this study) in an Arctic sediment core (PS1533, Tütken et al., 2002) over the last 140 ka was attributed to changes in the relative proportion of sediment derived from two isotopically distinct sources (Svalbard and Siberia) over glacial-interglacial cycles. Although the broad end-member identification will unlikely be affected, the calculated proportions of each end-member at different points in time would change if the those end-members were not constant over glacial-interglacial cycles.

6 Conclusions

The large variations in ^{87}Sr/^{86}Sr and εNd observed in sediments from two small catchments in Svalbard can be explained as a result of two isotopically and geochemically distinct sediment sources mixing during the Meoszoic and subsequently forming the Paleocene-Eocene sedimentary formations which are eroding today (Fig. 10). The two original sources are an eastern

sediment source derived from basaltic rocks from Siberia and a western sediment source derived from basement rocks from Greenland. The original geology of the sources controls the initial geochemistry, Sr and Nd isotope values and subsequently determines the type of clay minerals formed during weathering, susceptibility to later diagenesis and particle-size transport effects. Thus sedimentary processes in the past have influenced the Sr and Nd isotopic composition of the present formations.

5   In the modern day, changes in erosion caused by the glaciation of Dryadbreen has led to material from the upper (younger) formation, which contains a higher proportion of material derived from the western source, being moved lower down in the catchment where it is present in the moraines and sandur plain. In contrast, the lower (older) formation, which contains a higher proportion of material derived from the eastern source, is fully exposed in the unglaciated catchment, having not been covered by sediment from the upper formations of the catchment. This leads to a marked difference in the suspended sediment

10   export from the two catchments and suggests that changes in continental erosion during glacial-interglacial cycles could have a pronounced effect on the Sr and Nd isotopic composition of sediment exported from sedimentary catchments where those sediments have a complex history of multiple sources and sedimentary cycles. Given that the majority of the main rivers in the circum-Arctic region drain shale, the temporal variation of ^{87}Sr/^{86}Sr and εNd exported to the ocean from a given region over glacial-interglacial periods, may not have been constant. Further changes on the continents occurring during glacial-interglacial

15   cycles (hydrology, basin configuration) should also be considered as factors affecting εNd variation in ocean sediments.

Data availability. All data used in this manuscript is contained in the included tables apart from XRD data files. For data related queries, please contact the corresponding author.

Competing interests. The authors declare no competing interests.

Acknowledgements. This project was funded by a Swiss National Science Foundation fellowship for prospective researchers (PBEZP2-
20   137335), a Marie Curie Intra-European Fellowship (PIEF-GA-2012-331501), and NERC Standard Grant NE/M001865/1. Fieldwork was supported by an Arctic Field Grant (219165/E10, The Research Council of Norway). We wish to thank the fieldwork team and everyone who made the fieldwork possible, Angus Calder (University of St. Andrews) for help with XRD analysis, Chris Jeans (University of Cambridge) for help with the semi-quantitative analysis of clay minerals by XRD and Tim Heaton (British Geological Survey) for performing the stream suspended sediment leaches. We thank the two reviewers for their comments which have helped to considerably improve this manuscript.

References

Arndt, N. T. and Goldstein, S. L.: Use and abuse of crust-formation ages, Geology, 15, 893–895, 1987.

Aubert, D., Stille, P., and Probst, A.: REE fractionation during granite weathering and removal by waters and suspended loads: Sr and Nd isotopic evidence, Geochim. Cosmochim. Acta, 65, 387–406, 2001.

5 Awwiller, D. N.: Geochronology and mass transfer in Gulf Coast mudrocks (south-central Texas, U.S.A.): Rb-Sr, Sm-Nd and REE systematics, Chem. Geol., 116, 61–84, 1994.

Awwiller, D. N. and Mack, L. E.: Diagenetic modification of Sm-Nd model ages in Tertiary sandstones and shales, Texas Gulf Coast, Geology, 19, 311–314, 1991.

Babechuk, M. G., Widdowson, M., Murphy, M., and Kamber, B. S.: A combined Y/Ho, high field strength element (HFSE) and Nd isotope
10 perspective on basalt weathering, Deccan Traps, India, Chem. Geol., 369, 25–41, 2015.

Bayon, G., Toucanne, S., Skonieczny, C., André, L., Bermell, S., Cheron, S., Dennielou, B., Etoubleau, J., Freslon, N., Gauchery, T., Germain, Y., Jorry, S. J., Ménot, G., Monin, L., Ponzevera, E., Rouget, M.-L., Tachikawa, K., and Barrat, J. A.: Rare earth elements and neodymium isotopes in world river sediments revisited, Geochim. Cosmochim. Acta, 170, 17–38, https://doi.org/10.1016/j.gca.2015.08.001, 2015.

Bernstein, S., Kelemen, P. B., Tegner, C., Kurz, M. D., Blusztajn, J., and Brooks, C. K.: Post-breakup basaltic magmatism along the East
15 Greenland Tertiary rifted margin, Earth Planet. Sci. Lett., 160, 845–862, 1998.

Bock, B., McLennan, S. M., and Hanson, G. N.: Rare earth element redistribution and its effects on the neodymium isotope system in the Austin Glen Member of the Normanskill Formation, New York, USA, Geochim. Cosmochim. Acta, 58, 5245–5253, 1994.

Bue, E. P. and Andresen, A.: Constraining depositional models in the Barents Sea region using detrital zircon U-Pb data from Mesozoic sediments in Svalbard, in: Sediment provenance studies in hydrocarbon exploration and production, edited by Scott, R. A., Smyth, H. R.,
20 Morton, A. C., and Richardson, N., no. 386 in Special Publications, pp. 261–279, Geological Society, 2014.

Bullen, T., White, A., Blum, A., Harden, J., and Schulz, M.: Chemical weathering of a soil chronosequence on granitoid alluvium: II. Mineralogic and isotopic constraints on the behavior of strontium, Geochim. Cosmochim. Acta, 61, 291–306, 1997.

Burton, K. W. and Vance, D.: Glacial-interglacial variations in the neodymium isotope composition of seawater in the Bay of Bengal recorded by planktonic foraminifera, Earth Planet. Sci. Lett., 176, 425–441, 2000.

25 Byrne, R. H. and Kim, K.-H.: Rare earth element scavenging in seawater, Geochim. Cosmochim. Acta, 54, 2645–2656, 1990.

Byrne, R. H. and Sholkovitz, E. R.: Marine chemistry and geochemistry of the lanthanides, in: Handbook on the Physics and Chemistry of Rare Earths, edited by Gschneidner, Jr., K. A. and Eyring, L., vol. 23, chap. 158, pp. 497–593, Elsevier Science B. V., 1996.

Cameron, E. M. and Hattori, K.: Strontium and neodymium isotope ratios in the Fraser River, British Columbia: a riverine transect across the Cordilleran orogen, Chem. Geol., 137, 243–253, 1997.

30 Charles, A. J., Condon, D. J., Harding, I. C., Pälike, H., Marshall, J. E. A., Cui, Y., Kump, L., and Croudace, I. W.: Constraints on the numerical age of the Paleocene-Eocene boundary, Geochem. Geophys. Geosys., 12, Q0AA17, https://doi.org/10.1029/2010GC003426, 2011.

Chester, R. and Hughes, M. J.: A chemical technique for the separation of ferro-manganese minerals, carbonate minerals and adsorbed trace elements from pelagic sediments, Chem. Geol., 2, 249–262, 1967.

35 Clinger, A. E., Aciego, S. M., Stevenson, E. I., Arendt, C. A., and Robbins, M. J.: Implications for post-comminution processes in subglacial suspended sediment using coupled radiogenic strontium and neodymium isotopes, Geomorphology, 259, 134–144, https://doi.org/10.1016/j.geomorph.2016.02.006, 2016.

Collerson, K. D., McCulloch, M. T., and Nutman, A. P.: Sr and Nd isotope systematics of polymetamorphic Archean gneisses from southern West Greenland and northern Labrador, Can J. Earth Sci., 26, 446–466, 1989.

Cui, Y., Kump, L. R., Ridgwell, A. J., Charles, A. J., Junium, C. K., Diefendorf, A. F., Freeman, K. H., Urban, N. M., and Harding, I. C.: Slow release of fossil carbon during the Palaeocene–Eocene Thermal Maximum, Nat. Geosci., 4, 481–485, 2011.

5   Cullers, R. L., Bock, B., and Guidotti, C.: Elemental distributions and neodymium isotopic compositions of Silurian metasediments, western Maine, USA: Redistribution of the rare earth elements, Geochim. Cosmochim. Acta, 61, 1847–1861, 1997.

Curtin, D. and Smillie, G. W.: Composition and origin of smectite in soils derived from basalt in Northern Ireland, Clay Clay Miner., 29, 277–284, 1981.

Dasch, E. J.: Strontium isotopes in weathering profiles, deep-sea sediments, and sedimentary rocks, Geochim. Cosmochim. Acta, 33, 1521–
10   1552, 1969.

Dypvik, H., Riber, L., Burca, F., Rüther, D., Jargvoll, D., Nagy, J., and Jochmann, M.: The Paleocene-Eocene thermal maximum (PETM) in Svalbard - clay mineral and geochemical signals, Palaeogeogr. Palaeoclimatol. Palaeoecol., 302, 156–169, 2011.

Eisenhauer, A., Meyer, H., Rachold, V., Tütken, T., Wiegand, B., Hansen, B. T., Spielhagen, R. F., Lindemann, F., and Kassens, H.: Grain size separation and sediment mixing in Arctic Ocean sediments: evidence from the strontium isotope systematic, Chem. Geol., 158, 173–188,
15   1999.

Elling, F. J., Spiegel, C., Estrada, S., Davis, D. W., Reinhardt, L., Henjes-Kunst, F., Allroggen, N., Dohrmann, R., Piepjohn, K., and Lisker, F.: Origin of bentonites and detrital zircons of the Paleocene Basilika Formation, Svalbard, Front. Earth Sci., 4, 73, https://doi.org/10.3389/feart.2016.00073, 2016.

Essington, M. E.: Soil and Water Chemistry: An Integrative Approach, CRC Press, 2004.

20   Fagel, N., Not, C., Gueibe, J., Mattielli, N., and Bazhenova, E.: Late Quaternary evolution of sediment provenances in the Central Arctic Ocean: mineral assemblage, trace element composition and Nd and Pb isotope fingerprints of detrital fraction from the Northern Mendeleev Ridge, Quaternary Sci. Rev., 92, 140–154, 2014.

Friend, C. R. L., Nutman, A. P., Baadsgaard, H., and Duke, M. J. M.: The whole rock Sm-Nd 'age' for the 2825 Ma Ikkattoq gneisses (Greenland) is 800 Ma too young: Insights into Archaean TTG petrogenesis, Chem. Geol., 261, 62–76, 2009.

25   Garçon, M. and Chauvel, C.: Where is basalt in river sediments, and why does it matter?, Earth Planet. Sci. Lett., 407, 61–69, 2014.

Garçon, M., Chauvel, C., France-Lanord, C., Huyghe, P., and Lavé, J.: Continental sedimentary processes decouple Nd and Hf isotopes, Geochim. Cosmochim. Acta, 121, 177–195, 2013.

Gleason, J. D., Thomas, D. J., Moore Jr., T. C., Blum, J. D., Owen, R. M., and Haley, B. A.: Early to middle Eocene history of the Arctic Ocean from Nd-Sr isotopes in fossil fish debris, Lomonosov Ridge, Paleoceanography, 24, PA2215, https://doi.org/10.1029/2008PA001685,
30   2009.

Goldstein, S. L. and Jacobsen, S. B.: The Nd and Sr isotopic systematics of river-water dissolved material: Implications for the sources of Nd and Sr in seawater, Chem. Geol., 66, 245–272, 1987.

Goldstein, S. L. and Jacobsen, S. B.: Nd and Sr isotopic systematics of river water suspended material: Implications for crustal evolution, Earth Planet. Sci. Lett., 87, 249–265, 1988.

35   Govindaraju, K.: 1994 compilation of working values and sample descriptions for 383 geostandards, Geostandard. Newslett., 18, 1–158, 1994.

Griffin, G. M.: Interpretation of X-ray diffraction data, in: Procedures in sedimentary petrology, edited by Carver, R. E., pp. 541–569, Wiley-Interscience, New York, 1971.

Griffin, J. J., Windom, H., and Goldberg, E. D.: The distribution of clay minerals in the World Ocean, Deep-Sea Res., 15, 433–459, 1968.

Haley, B. A., Klinkhammer, G. P., and McManus, J.: Rare earth elements in pore waters of marine sediments, Geochim. Cosmochim. Acta, 68, 1265–1279, 2004.

Helland-Hansen, W.: Sedimentation in Paleogene Foreland Basin, Spitsbergen, AAPG Bull., 74, 260–272, 1990.

5   Henriksen, N.: Conclusion of the 1:500 000 mapping project in the Caledonian fold belt in North-East Greenland, in: Review of Greenland activities 1998, edited by Higgins, A. K. and Watt, W. S., vol. 183 of Geology of Greenland Survey Bulletin, pp. 10–22, GEUS, 1999.

Herron, M. M.: Geochemical classification of terrigenous sands and shales from core or log data, J. Sediment. Petrol., 58, 820–829, 1988.

Hillaire-Marcel, C., Maccali, J., Not, C., and Poirier, A.: Geochemical and isotopic tracers of Arctic sea ice sources and export with special attention to the Younger Dryas interval, Quaternary Sci. Rev., 79, 184–190, 2013.

10   Hindshaw, R. S.: Chemical weathering and calcium isotope fractionation in a glaciated catchment, Ph.D. thesis, ETH Zurich, 2011.

Hindshaw, R. S., Heaton, T. H. E., Boyd, E. S., Lindsay, M. R., and Tipper, E. T.: Influence of glaciation on mechanisms of mineral weathering in two high Arctic catchments, Chem. Geol., 420, 37–50, https://doi.org/10.1016/j.chemgeo.2015.11.004, 2016.

Humlum, O., Instanes, A., and Sollid, J. L.: Permafrost in Svalbard: a review of research history, climatic background and engineering challenges, Polar Res., 22, 191–215, https://doi.org/10.3402/polar.v22i2.6455, 2003.

15   Jacobsen, S. B.: Isotopic constraints on crustal growth and recycling, Earth Planet. Sci. Lett., 90, 315–329, 1988.

Jacobsen, S. B. and Wasserburg, G. J.: Sm-Nd isotopic evolution of chondrites, Earth Planet. Sci. Lett., 50, 139–155, 1980.

Jakobsson, M., Backman, J., Rudels, B., Nycander, J., Frank, M., Mayer, L., Jokat, W., Sangiorgi, F., O'Regan, M., Brinkhuis, H., King, J., and Moran, K.: The early Miocene onset of a ventilated circulation regime in the Arctic Ocean, Nature, 447, 986–990, 2007.

Jeandel, C., Arsouze, T., Lacan, F., Téchiné, P., and Dutay, J.-C.: Isotopic Nd compositions and concentrations of the lithogenic inputs into

20   the ocean: a compilation, with an emphasis on the margins, Chem. Geol., 239, 156–164, 2007.

Johannesson, K. H. and Zhou, X.: Origin of middle rare earth element enrichments in acid waters of a Canadian High Arctic Lake, Geochim. Cosmochim. Acta, 63, 153–165, 1999.

Johansson, Å. and Gee, D. G.: The late Palaeoproterozoic Eskolabreen granitoids of southern Ny Friesland, Svalbard Caledonides - geo-chemistry, age, and origin, GFF, 121, 113–126, 1999.

25   Johansson, Å., Gee, D. G., Björklund, L., and Witt-Nilsson, P.: Isotope studies of granitoids from the Bangenhuk Formation, Ny Friesland Caledonides, Svalbard, Geol. Mag., 132, 303–320, 1995.

Jones, M. T., Eliassen, G. T., Shephard, G. E., Svensen, H. H., Jochmann, M., Friis, B., Augland, L. E., Jerram, D. A., and Planke, S.: Provenance of bentonite layers in the Paleocene strata of the Central Basin, Svalbard: implications for magmatism and rifting events around the onset of the North Atlantic Igneous Province, J. Volcan. Geo. Res., 327, 571–584, 2016.

30   Kalsbeek, F. and Frei, R.: The Mesoproterozoic Midsommersø dolerites and associated high-silica intrusions, North Greenland: crustal melting, contamination and hydrothermal alteration, Contrib. Mineral. Petrol., 152, 89–110, 2006.

Knies, J. and Gaina, C.: Middle Miocene ice sheet expansion in the Arctic: Views from the Barents Sea, Geochem. Geophys. Geosyst., 9, Q02 015, 2008.

Knies, J., Mattingsdal, R., Fabian, K., Grøsfjeld, K., Baranwal, S., Husum, K., De Schepper, S., Vogt, C., Andersen, N., Matthiessen, J.,

35   Andreassen, K., Jokat, W., Nam, S.-I., and Gaina, C.: Effect of early Pliocene uplift on late Pliocene cooling in the Arctic-Atlantic gateway, Earth Planet. Sci. Lett., 387, 132–144, 2014.

Krogstad, E. J., Fedo, C. M., and Eriksson, K. A.: Provenance ages and alteration histories of shales from the Middle Archean Buhwa greenstone belt, Zimbabwe: Nd and Pb isotopic evidence, Geochim. Cosmochim. Acta, 68, 319–332, 2004.

Lightfoot, P. C., Hawkesworth, C. J., Hergt, J., Naldrett, A. J., Gorbachev, N. S., Fedorenko, V. A., and Doherty, W.: Remobilisation of the continental lithosphere by a mantle plume: major-, trace-element, and Sr-, Nd-, and Pb-isotope evidence from picritic and tholeiitic lavas of the Noril'sk District, Siberian Trap, Russia, Contrib. Mineral. Petrol., 114, 171–188, 1993.

Lupker, M., France-Lanord, C., Galy, A., Lavé, J., and Kudrass, H.: Increasing chemical weathering in the Himalayan system since the Last Glacial Maximum, Earth Planet. Sci. Lett., 365, 243–252, 2013.

Ma, J., Wei, G., Xu, Y., and Long, W.: Variations of Sr-Nd-Hf isotopic systematics in basalt during intensive weathering, Chem. Geol., 269, 376–385, 2010.

Maccali, J., Hillaire-Marcel, C., Carignan, J., and Reisberg, L. C.: Geochemical signatures of sediments documenting Arctic sea-ice and water mass export through Fram Strait since the Last Glacial Maximum, Quaternary Sci. Rev., 64, 136–151, https://doi.org/10.1016/j.quascirev.2012.10.029, 2013.

Major, H., Haremo, P., Dallmann, W. K., and Andresen, A.: Geological map of Svalbard 1:100 000, sheet C9G Adventdalen, Temakart nr. 31, Norsk Polarinstitutt, Tromsø, Norway, 2000.

McCulloch, M. T. and Wasserburg, G. J.: Sm-Nd and Rb-Sr chronology of continental crust formation, Science, 200, 1003–1011, 1978.

McLennan, S. M., McCulloch, M. T., Taylor, S. R., and Maynard, J. B.: Effects of sedimentary sorting on neodymium isotopes in deep-sea turbidites, Nature, 337, 547–549, 1989.

Meinhardt, A.-K., Pahnke, K., Böning, B., Schnetger, B., and Brumsack, H.-J.: Climate change and response in bottom water circulation and sediment provenance in the Central Arctic Ocean since the Last Glacial, Chem. Geol., 427, 98–108, 2016.

Millero, F. J.: Stability constants for the formation of rare earth inorganic complexes as a function of ionic strength, Geochim. Cosmochim. Acta, 56, 3123–3132, 1992.

Mokadem, F., Parkinson, I. J., Hathorne, E. C., Anand, P., Allen, J. T., and Burton, K. W.: High-precision radiogenic strontium isotope measurements of the modern and glacial ocean: Limits on glacial-interglacial variations in continental weathering, Earth Planet. Sci. Lett., 415, 111–120, https://doi.org/10.1016/j.epsl.2015.01.036, 2015.

Moore, D. M. and Reynolds Jr., R. C.: X-ray diffraction and the identification and analysis of clay minerals, Oxford University Press, New York, 1997.

Müller, R. D. and Spielhagen, R. F.: Evolution of the Central Tertiary Basin of Spitsbergen: towards a synthesis of sediment and plate tectonic history, Palaeogeogr. Palaeoclimatol. Palaeoecol., 80, 153–172, 1990.

Nordli, Ø., Przybylak, R., Ogilvie, A. E. J., and Isaksen, K.: Long-term temperature trends and variability on Spitsbergen: the extended Svalbard Airport temperature series, 1898-2012, Polar Res., 33, 21 349, https://doi.org/10.3402/polar.v33.21349, 2012.

Nürnberg, D., Wollenburg, I., Dethleff, D., Eicken, H., Kassens, H., Letzig, T., Reimnitz, E., and Thiede, J.: Sediments in Arctic sea ice: Implications for entrainment, transport and release, Marine Geology, 119, 185–214, 1994.

Öhlander, B., Ingri, J., Land, M., and Schöberg, H.: Change of Sm-Nd isotope composition during weathering of till, Geochim. Cosmochim. Acta, 64, 813–820, 2000.

Ohr, M., Halliday, A. N., and Peacor, D. R.: Sr and Nd isotopic evidence for punctuated clay diagenesis, Texas Gulf Coast, Earth Planet. Sci. Lett., 105, 110–126, 1991.

Ohr, M., Halliday, A. N., and Peacor, D. R.: Mobility and fractionation of rare earth elements in argillaceous sediments: Implications for dating diagenesis and low-grade metamorphism, Geochim. Cosmochim. Acta, 58, 289–312, 1994.

Parra, M., Delmont, P., Ferragne, A., Latouche, C., Pons, J. C., and Puechmaille, C.: Origin and evolution of smectites in recent marine sediments of the NE Atlantic, Clay Miner., 20, 335–346, 1985.

Pearce, C. R., Jones, M. T., Oelkers, E. H., Pradoux, C., and Jeandel, C.: The effect of particulate dissolution on the neodymium (Nd) isotope and Rare Earth Element (REE) composition of seawater, Earth Planet. Sci. Lett., 369-370, 138–147, 2013.

Petersen, T. G., Thomsen, T. B., Olaussen, S., and Stemmerik, L.: Provenance shifts in an evolving Eurekan foreland basin: the Tertiary Central Basin, Spitsbergen, J. Geol. Soc., 173, 634–648, https://doi.org/10.1144/jgs2015-076, 2016.

5 Peucker-Ehrenbrink, B., Miller, M. W., Arsouze, T., and Jeandel, C.: Continental bedrock and riverine fluxes of strontium and neodymium isotopes to the oceans, Geochem. Geophys. Geosys., 11, Q03 016, https://doi.org/10.1029/2009GC002869, 2010.

Piotrowski, A. M., Banakar, V. K., Scrivner, A. E., Elderfield, H., Galy, A., and Dennis, A.: Indian Ocean circulation and productivity during the last glacial cycle, Earth Planet. Sci. Lett., 285, 179–189, 2009.

Raczek, I., Stoll, B., Hofmann, A. W., and Jochum, K. P.: High-precision trace element data for the USGS reference materials BCR-1,
10   BCR-2, BHVO-1, BHVO-2, AGV-1, AGV-2, DTS-1, DTS-2, GSP-1 and GSP-2 by ID-TIMS and MIC-SSMS, Geostandard. Newslett., 25, 77–86, 2001.

Rickli, J., Frank, M., Stichel, T., Georg, R. B., Vance, D., and Halliday, A. N.: Controls on the incongruent release of hafnium during weathering of metamorphic and sedimentary catchments, Geochim. Cosmochim. Acta, 101, 263–284, 2013.

Rickli, J., Hindshaw, R. S., Leuthold, J., Wadham, J. L., Burton, K. W., and Vance, D.: Impact of glacial activity on the weathering of Hf
15   isotopes - observations from Southwest Greenland, Geochim. Cosmochim. Acta, 215, 295–316, 2017.

Schlegel, A., Lisker, F., Dörr, N., Jochmann, M., Schubert, K., and Spiegel, C.: Petrography and geochemistry of siliclastic rocks from the Central Tertiary Basin of Svalbard - implications for provenance, tectonic setting and climate, Z. Dt. Ges. Geowiss., 164, 173–186, 2013.

Setti, M., Marinoni, L., and López-Galindo, A.: Mineralogical and geochemical characteristics (major, minor, trace elements and REE) of detrital and authigenic clay minerals in a Cenozoic sequence from Ross Sea, Antarctica, Clay Miner., 39, 405–421,
20   https://doi.org/10.1180/000985503540143, 2004.

Singer, A.: The paleoclimatic interpretation of clay minerals in sediments - a review, Earth Sci. Rev., 21, 251–293, 1984.

Sionneau, T., Bout-Roumazeilles, V., Biscaye, P. E., Van Vliet-Lanoe, B., and Bory, A.: Clay mineral distributions in and around the Mississippi River watershed and Northern Gulf of Mexico: sources and transport patterns, Quaternary Sci. Rev., 27, 1740–1751, 2008.

Spadea, P. and D'Antonio, M.: Initiation and evolution of intra-oceanic subduction in the Uralides: Geochemical and isotopic constraints
25   from Devonian oceanic rocks of the Southern Urals, Russia, Island Arc, 15, 7–25, 2006.

Spielhagen, R. F., Baumann, K.-H., Erlenkeuser, H., Nowaczyk, N. R., Nørgaard-Pedersen, N., Vogt, C., and Weiel, D.: Arctic ocean deep-sea record of northern Eurasian ice sheet history, Quaternary Sci. Rev., 23, 1455–1483, 2004.

Su, N., Yang, S., Guo, Y., Yue, W., Wang, X., Yin, P., and Huang, X.: Revisit of rare earth element fractionation during chemical weathering and river sediment transport, Geochem. Geophys. Geosys., 18, 935–955, https://doi.org/10.1002/2016GC006659, 2017.

30 Svendsen, J. I. and Mangerud, J.: Holocene glacial and climatic variations on Spitsbergen, Svalbard, Holocene, 7, 45–57, https://doi.org/10.1177/095968369700700105, 1997.

Svendsen, J. I., Alexanderson, H., Astakhov, V. I., Demidov, I., Dowdeswell, J. A., Funder, S., Gataullin, V., Henriksen, M., Hjort, C., Houmark-Nielsen, M., Hubberten, H. W., Ingólfsson, O., Jakobsson, M., Kjær, K. H., Larsen, E., Lokrantz, H., Lunkka, J. P., Lyså, A., Mangerud, J., Matiouchkov, A., Murray, A., Möller, P., Niessen, F., Nikolskaya, O., Polyak, L., Saarnisto, M., Siegert, C., Siegert, M. J.,
35   Spielhagen, R. F., and Stein, R.: Late Quaternary ice sheet history of northern Eurasia, Quaternary Sci. Rev., 23, 1229–1271, 2004.

Tanaka, T., Togashi, S., Kamioka, H., Amakawa, H., Kagami, H., Hamamoto, T., Yuhara, M., Orihashi, Y., Yoneda, S., Shimizu, H., Kunimaru, T., Takahashi, K., Yanagi, T., Nakano, T., Fujimaki, H., Shinjo, R., Asahara, Y., Tanimizu, M., and Dragusanu, C.: JNd-1: a neodymium isotopic reference in consistency with LaJolla neodymium, Chem. Geol., 168, 279–281, 2000.

Taylor, S. R. and McLennan, S. M.: The continental crust: Its composition and evolution, Blackwell Scientific, Boston, Mass., 1985.

Teller, J. T.: Volume and routing of late-glacial runoff from the southern Laurentide ice sheet, Quaternary Res., 34, 12–23, 1990.

Tepe, N. and Bau, M.: Importance of nanoparticles and colloids from volcanic ash for riverine transport of trace elements to the ocean: Evidence from glacial-fed rivers after the 2010 eruption of Eyjafjallajökull Volcano, Iceland, Sci. Tot. Environ., 488-489, 243–251, 2014.

5   Tessier, A., Campbell, P. G. C., and Bisson, M.: Sequential extraction procedure for the speciation of particulate trace metals, Anal. Chem., 51, 844–851, 1979.

Tricca, A., Stille, P., Steinmann, M., Kiefel, B., Samuel, J., and Eikenberg, J.: Rare earth elements and Sr and Nd isotopic compositions of dissolved and suspended loads from small river systems in the Vosges mountains (France), the river Rhine and groundwater, Chem. Geol., 160, 139–158, 1999.

10 Tütken, T., Eisenhauer, A., Wiegand, B., and Hansen, B. T.: Glacial-interglacial cycles in Sr and Nd isotopic composition of Arctic marine sediments triggered by the Svalbard/Barents Sea ice sheet, Marine Geology, 182, 351–372, 2002.

Veizer, J.: Chemical diagenesis of carbonates: theory and application of trace element technique, in: Stable isotopes in sedimentary geology, edited by Arthur, M. A., Anderson, T. F., Kaplan, I. R., Veizer, J., and Land, L. S., vol. 10, pp. 3–1–3–100, Society of Economic Paleontologists and Mineralogists Short Course Notes, 1983.

15 Viers, J. and Wasserburg, G. J.: Behavior of Sm and Nd in a lateritic soil profile, Geochim. Cosmochim. Acta, 68, 2043–2054, https://doi.org/10.1016/j.gca.2003.10.034, 2004.

Viers, J., Roddaz, M., Filizola, N., Guyot, J.-L., Sondag, F., Brunet, P., Zouiten, C., Boucayrand, C., Martin, F., and Boaventura, G. R.: Seasonal and provenance controls on Nd-Sr isotopic compositions of Amazon rivers suspended sediments and implications for Nd and Sr fluxes exported to the Atlantic Ocean, Earth Planet. Sci. Lett., 274, 511–523, 2008.

20 Vogt, C., Knies, J., Spielhagen, R. F., and Stein, R.: Detailed mineralogical evidence for two nearly identical glacial/interglacial cycles and Atlantic water advection to the Arctic Ocean during the last 90,000 years, Global Planet. Change, 31, 23–44, 2001.

von Blanckenburg, F. and Nägler, T. F.: Weathering versus circulation-controlled changes in radiogenic isotope tracer composition of the Labrador Sea and North Atlantic Deep Water, Paleoceanography, 16, 424–434, 2001.

Vonk, J. E., Giosan, L., Blusztajn, J., Montlucon, D., Pannatier, E. G., McIntyre, C., Wacker, L., Macdonald, R. W., Yunker, M. B., and Eglinton, T. I.: Spatial variations in geochemical characteristics of the modern Mackenzie Delta sedimentary system, Geochim. Cosmochim. Acta, 171, 100–120, 2015.

Wahsner, M., Müller, C., Stein, R., Ivanov, G., Levitan, M., Shelekhova, E., and Tarasov, G.: Clay-mineral distribution in surface sediments of the Eurasian Arctic Ocean and continental margin as indicator for source areas and transport pathways - a synthesis, Boreas, 28, 215–232, 1999.

30 Weis, D., Demaiffe, D., Souchez, R., Gow, A. J., and Meese, D. A.: Ice sheet development in Central Greenland: implications from the Nd, Sr and Pb isotopic compositions of basal material, Earth Planet. Sci. Lett., 150, 161–169, 1997.

Wickert, A. D.: Reconstruction of North American drainage basins and river discharge since the Last Glacial Maximum, Earth Surf. Dynam., 4, 831–869, https://doi.org/10.5194/esurf-4-831-2016, 2016.

Wilson, D. J., Piotrowski, A. M., Galy, A., and Clegg, J. A.: Reactivity of neodymium carriers in deep sea sediments: Implications for boundary exchange and paleoceanography, Geochim. Cosmochim. Acta, 109, 197–221, 2013.

35 Winkler, A., Wolf-Welling, T. C. W., Stattegger, K., and Thiede, J.: Clay mineral sedimentation in high northern latitude deep-sea basins since the Middle Miocene (ODP Leg 151, NAAG), Int. J. Earth Sci., 91, 133–148, 2002.

Wooden, J. L., Czamanske, G. K., Fedorenko, V. A., Arndt, N. T., Chauvel, C., Bouse, R. M., King, B.-S. W., Knight, R. J., and Siems, D. F.: Isotopic and trace-element constraints on mantle and crustal contributions to Siberian continental flood basalts, Noril'sk area, Siberia, Geochim. Cosmochim. Acta, 57, 3677–3704, 1993.

Ziaja, W. and Pipała: Glacial recession 2001-2006 and its landscape effects in the Lindströmfjellet-Håbergnuten mountain ridge, Nordenskiöld Land, Spitsbergen, Pol. Polar Res., 28, 237–247, 2007.
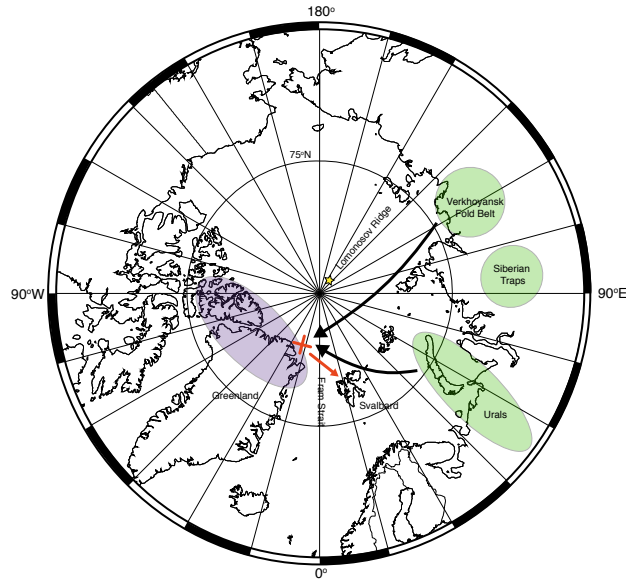
Figure 1. Overview of the circum-Arctic region. The red cross indicates the position of Svalbard during the Paleogene (Jones et al., 2016). The purple shaded area indicates the western shield source whilst the green circles indicate potential basaltic source regions in the east. The yellow star indicates the location of the Gleason et al. (2009) study to recover Eocene seawater compositions referred to in the text.
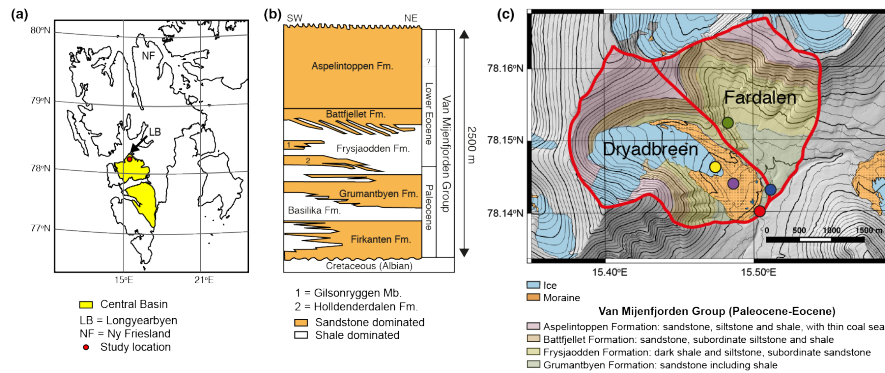
Figure 2. (**a**) Map of Svalbard indicating the extent of the Paleogene Central Basin. The location of the study area in relation to Longyearbyen is also indicated. (**b**) The stratigraphy of the Van Mijenfjorden Group adapted from Cui et al. (2011). The catchments are located at the NE side. (**c**) Topographic map of the sediment sampling locations with the geology of the catchments superimposed. Glaciers and their moraines are shown in blue and orange respectively and contours are displayed at 50 m intervals. The ~~red dashed~~ solid red lines demarcate the catchment boundaries. Dryadbreen is on the left and Fardalen on the right. The coloured circles indicate where samples referred to in Table 1 were collected: R01 and G (green circle); supraglacial stream suspended sediment sample, R03, R04 and D (yellow); Fardalen stream suspended sediment sample and L (blue); Dryadbreen stream suspended sediment sample and O (red); R02 (purple). Other rock and sediment samples referred to in Table 2 were collected at various locations within the two catchments. Geological information is taken from (Major et al., 2000) and the topographic information is based on GIS data from the Norwegian Polar Institute.
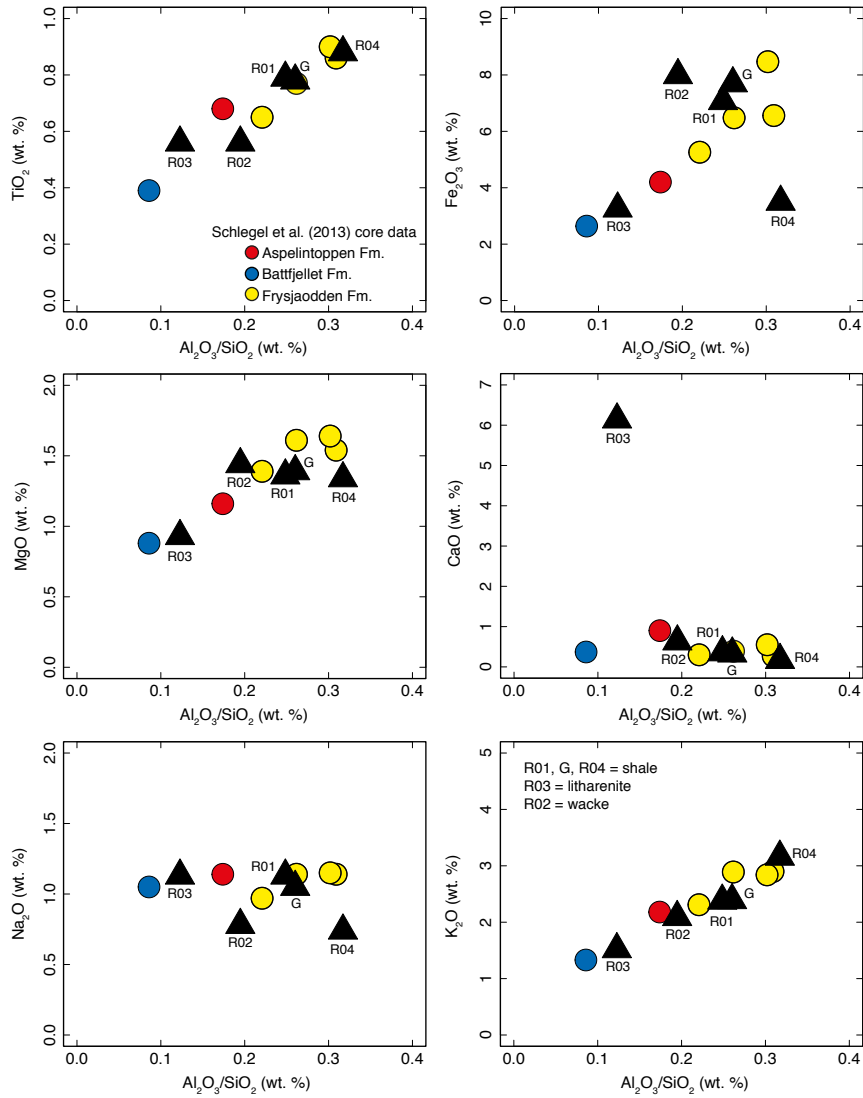
Figure 3. Plots of major elements in the collected rock samples against the Al₂O₃/SiO₂ ratio compared with core data (Store Norske Well 11-2003) covering the same formations (Schlegel et al., 2013). Sample R03 contains 10% carbonate, accounting for the high Ca concentration (Hindshaw et al., 2016).
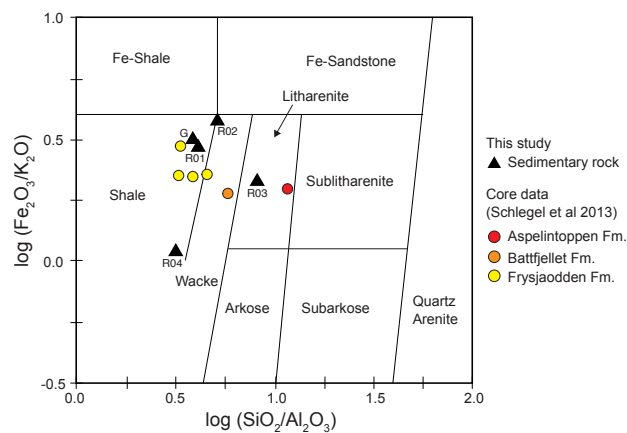
Figure 4. Herron classification (Herron, 1988) of the sedimentary rock samples collected in this study and from the core analysed by Schlegel et al. (2013). Samples G and R01 were collected in the unglaciated catchment (Fardalen) directly from the Frysjaodden Formation. Samples R03, R02 and R04 were collected in the glaciated catchment (Dryadbreen) but could not be linked to a specific formation in the field due to the heterogeneous nature of moraine material. Based on this classification and the major element chemistry (Fig. 3) we infer that R03 was derived from the Aspelintoppen Formation and R02 close to the Battfjellet/Frysjaodden boundary. Sample R04 is classified as a shale but has a markedly different iron content (Fig. 3) to the shale samples from the Frysjaodden Formation (R01, G). Based on its sampled location on the surface of the glacier we infer that it is a shale from either the Battfjellet or Aspelintoppen Formation (Fig. 2c).
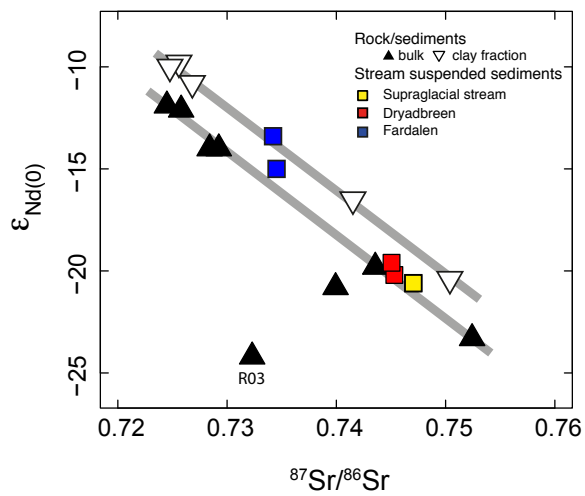
Figure 5. A plot of $^{87}Sr/^{86}Sr$ vs εNd. The grey lines highlight the parallel trends of the bulk and the clay-sized fraction data. Sample R03 is a litharenite whereas the other samples are predominantly shale (Table 1).
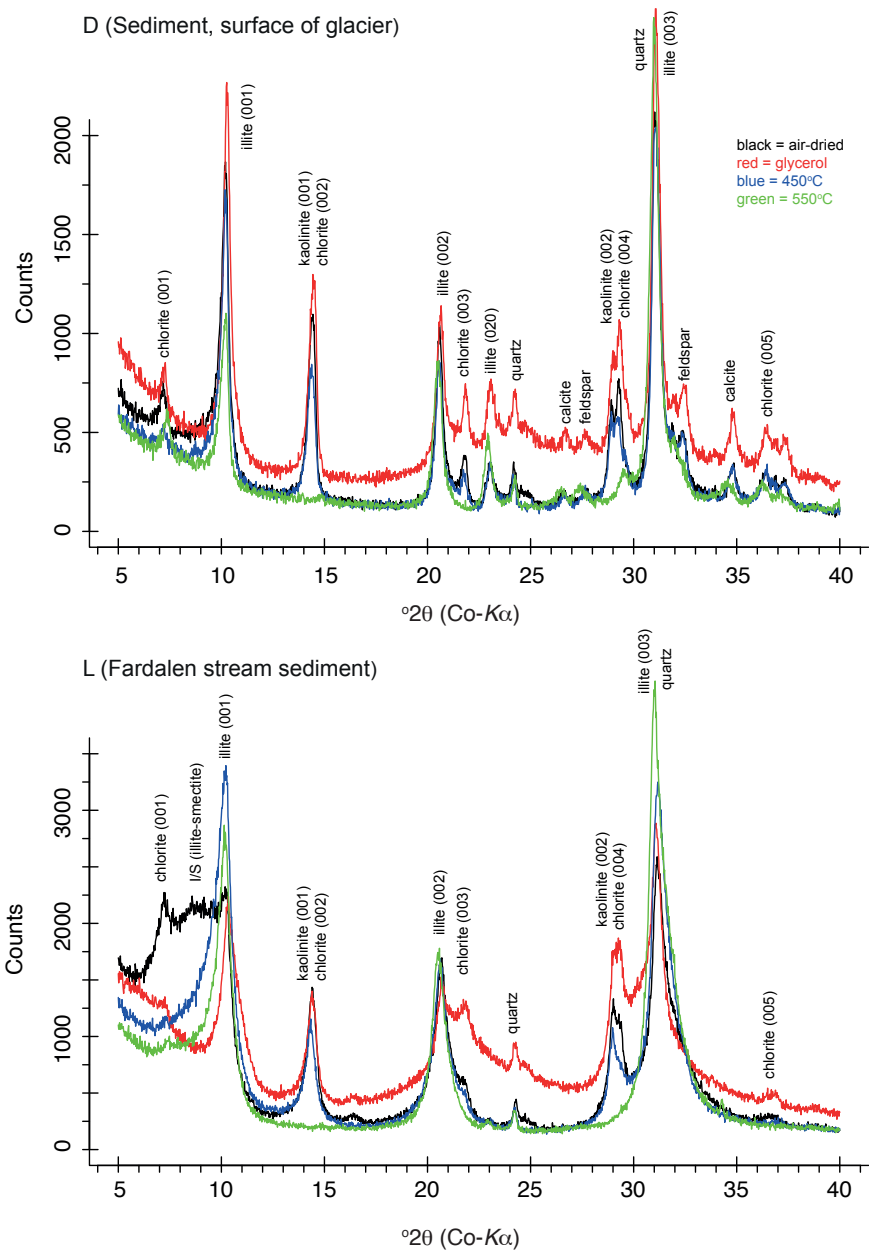
Figure 6. XRD patterns from two different samples: one with a high relative illite abundance (D) and one with low relative illite abundance and the clear presence of an expandable clay, likely an illite-smectite (I/S) mixed phase mineral (L).
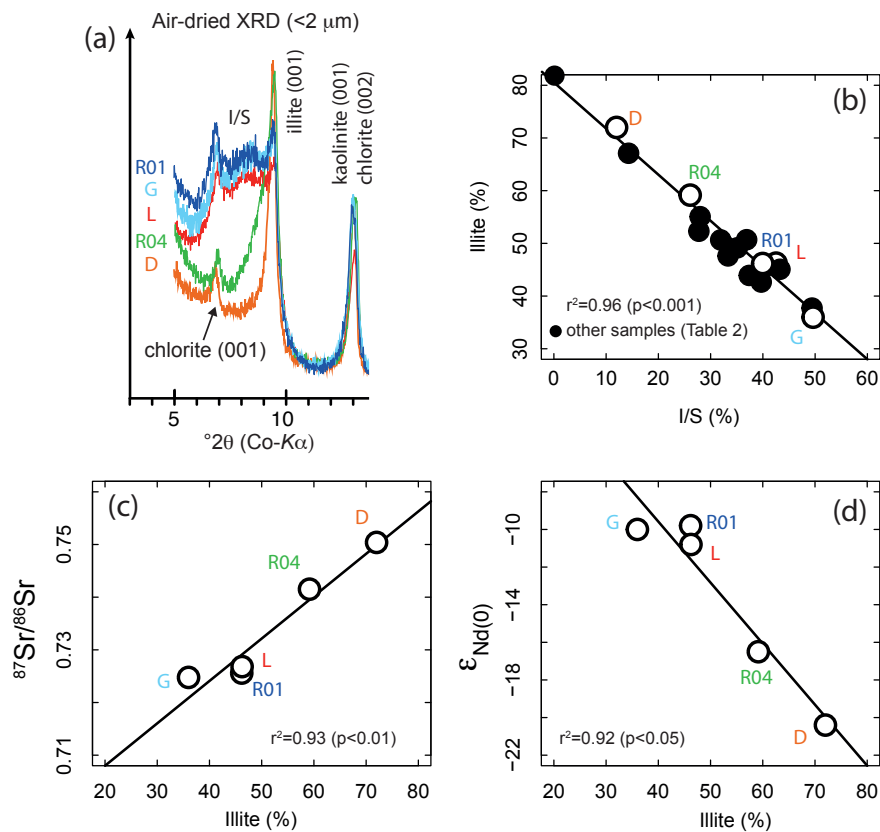
Figure 7. (**a**) Part of the orientated clay XRD spectrum (air-dried) for five samples. I/S stands for a mixed layer clay containing smectite and illite. Note the decrease in the I/S peak from R01 to D. (**b**) The relative abundances of illite and I/S in the clay fraction are inversely correlated. (**c,d**) There is a positive correlation between the relative abundance of illite and the radiogenic strontium isotope ratio in the clay fraction and an inverse correlation with the radiogenic neodymium isotope ratio.
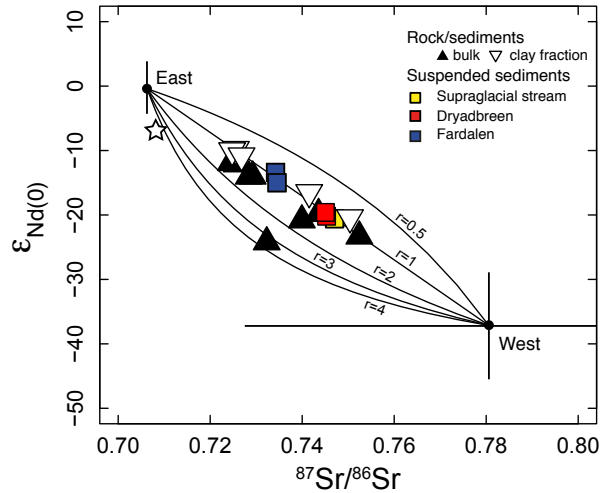
Figure 8. Plot of εNd vs ^{87}Sr/^{86}Sr. The two points 'East' (^{87}Sr/^{86}Sr = 0.70626, εNd = -0.4) and 'West' (^{87}Sr/^{86}Sr = 0.78059, εNd = -37.1) are averages of the interquartile range of literature data and the error bars indicate the interquartile range (for the 'East' source the error in ^{87}Sr/^{86}Sr is too small to see). 'East' data (n=99): Siberian Traps (Lightfoot et al., 1993; Wooden et al., 1993) and Uralides (Spadea and D'Antonio, 2006). 'West' data (n=65): Archaean rocks (predominantly gneisses, Jacobsen, 1988; Collerson et al., 1989; Kalsbeek and Frei, 2006; Friend et al., 2009), basal ice particles from GISP 2 and GRIP and granite bedrock samples from GISP 2 (Weis et al., 1997). The 'r' values are the Sr/Nd ratio of the 'East' source divided by the Sr/Nd ratio of the 'West' source. The star indicates the isotopic composition of Eocene seawater (Gleason et al., 2009, see text for details).
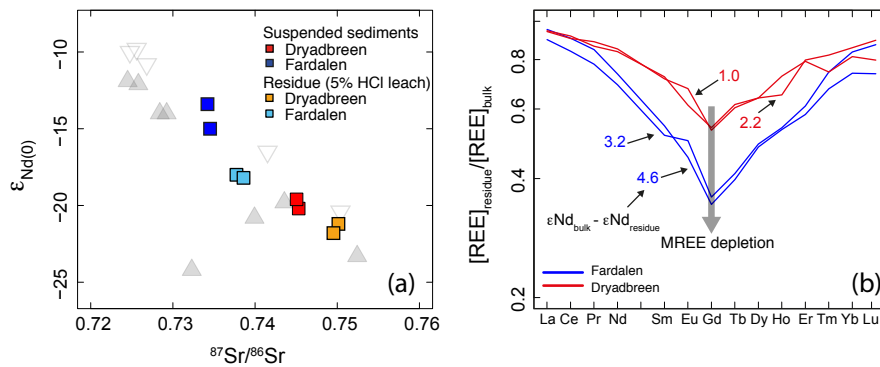
Figure 9. (**a**) εNd and ^{87}Sr/^{86}Sr data for bulk suspended sediments and residual suspended sediments after leaching with 5% HCl. In the background is the data from Fig. 5. (**b**) Rare earth element (REE) abundances of the residue relative to the bulk phase. The greater the depletion in middle REE (MREE), the greater the difference in εNd between bulk and residual phases and this difference is most pronounced in the unglaciated catchment (Fardalen) where relative I/S abundances are higher compared to the glaciated catchment (Dryadbreen, Table 2). The residual phases have a lower εNd value compared to the bulk.
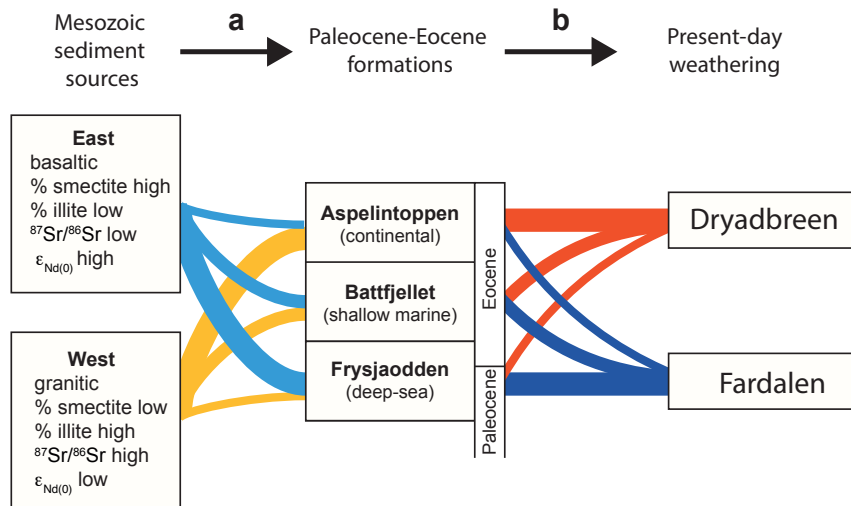
Figure 10. Summary of the processes leading to the variation in clay mineralogy, $^{87}Sr/^{86}Sr$ and εNd observed in the two studied catchments. The thickness of the lines gives an indication of the relative contribution of Mesozoic sources to Eocene formations and the Eocene formations to suspended sediment export from the two catchments. For example, the Frysjaodden Formation receives a greater proportion of sediment from the eastern source as compared to the western source. (**a**) The contribution of Meoszoic sediment sources to Eocene formations is determined by the depositional location (far-shore vs near-shore), particle size and susceptibility to authigenic phase formation. (**b**) The contribution of the Paleogene formations to the present-day suspended sediment load is determined by the present-day exposure of the formations in each catchment (Fig. 2) which is determined by the recent erosional history of the catchments.

Table 1. Major and selected trace metal concentrations, $^{87}Sr/^{86}Sr$ and εNd values for solid samples. Major elements (in wt%) were measured by ICP-OES and trace elements (mg/kg) were measured by ICP-MS. REE data are presented in Table A2.

Name and description	SSC[1] mg/L	SiO$_2$[2] wt%	Al$_2$O$_3$ wt%	Fe$_2$O$_3$ wt%	TiO$_2$ wt%	MgO wt%	CaO wt%	Na$_2$O wt%	K$_2$O wt%	P$_2$O$_5$ wt%	LOI wt%	Mn mg/kg	Ba mg/kg	Sr mg/kg	Rb mg/kg	Nd mg/kg	Sm mg/kg	$^{87}Sr/^{86}Sr$	2SD[4]	εNd	2SD[4]
Sedimentary rock samples																					
R01 = shale (pieces)		63.2	15.7	7.07	0.79	1.36	0.36	1.13	2.38	0.21	7.9	497	438	98	103	32	6	0.724490	17	-11.9	0.0
G = shale (pieces)		61.5	16.0	7.70	0.78	1.39	0.33	1.05	2.39	0.24	8.6	613	425	100	103	32	6	0.725796	28	-12.1	1.0
R04 = shale (rock)		58.3	18.5	3.50	0.88	1.34	0.17	0.74	3.16	0.09	13.3	190	542	107	147	39	7	0.743564	32	-19.8	0.7
R02 = wacke		64.7	12.6	7.99	0.56	1.44	0.63	0.78	2.09	0.26	8.9	1056	371	83	89	26	5	0.729241	22	-14.0	0.6
R03 = litharenite		70.0	8.6	3.26	0.56	0.93	6.14	1.13	1.52	0.11	7.7	480	366	139	54	25	5	0.732295	14	-24.2	0.2
Sediment sample																					
D = sediment (surface of glacier)		54.2	18.3	6.71	0.75	1.47	0.53	0.93	3.28	0.11	13.8	735	706	99	135	36	6	0.752425	36	-23.3	0.2
Stream sediment samples																					
L = stream sediment (Fardalen)		62.7	15.3	7.68	0.74	1.35	0.32	0.99	2.42	0.21	8.2	692	448	99	104	32	6	0.728400	77	-14.0	0.6
O = stream sediment (Dryadbreen)		69.3	11.2	5.09	0.69	1.03	0.44	1.11	1.94	0.18	9.0	568	448	78	76	33	6	0.739930	17	-20.8	0.6
<2 μm fraction fraction of bulk rock and sediment samples																					
R01-clay		49.6	20.7	9.26	0.65	1.70	0.48	2.08	3.14	1.99	9.6	452	451	82	142	38	8	0.725590	25	-9.8	0.5
G-clay		52.0	19.1	8.82	0.60	1.68	0.47	4.04	3.03	4.13	10.1	650	427	93	132	33	6	0.724766	27	-10.0	0.2
R04-clay		53.6	24.7	3.63	0.72	1.56	0.38	3.45	4.37	2.80	11.9	163	664	132	200	32	6	0.741518	18	-16.5	0.4
D-clay		57.6	24.4	6.30	0.64	1.49	0.43	4.45	4.37	3.81	11.8	526	828	120	186	26	5	0.750395	25	-20.4	0.2
L-clay		54.5	20.5	9.72	0.56	1.77	0.49	3.22	3.23	2.99	12.0	705	431	89	140	29	6	0.726819	28	-10.8	0.4
Stream suspended sediments (Bulk)																					
20120801SG[3]		47.7	16.4	5.72	0.74	1.35	0.34	0.90	3.00	0.14	19.1	482	687	98	123	34	6	0.747044	11	-20.6	0.5
20120617D[3]	62	43.8	19.2	6.51	0.75	1.54	0.45	1.02	3.45	0.17	10.7	660	1031	105	142	34	6	0.745052	51	-19.6	0.1
20120618F[3]	32	40.9	17.8	6.94	0.77	1.48	0.39	1.05	2.94	0.20	9.4	1227	738	108	128	40	8	0.734528	31	-15.0	0.2
20120726F[3]	19	43.2	18.0	7.04	0.76	1.55	0.42	1.04	3.07	0.22	11.1	769	595	115	130	42	9	0.734207	4	-13.4	0.4
20120729D[3]	404	47.1	21.0	7.37	0.82	1.77	0.49	0.89	3.68	0.21	10.9	660	756	114	162	37	7	0.745309	22	-20.2	0.5
Stream suspended sediments (Acid-treated)																					
20120617D(HCl)		43.9	20.2	6.44	0.73	1.45	0.06	1.04	3.56	0.07	10.3	366	1019	96	153	29	4	0.749536	3	-21.8	0.3
20120618F(HCl)		39.5	18.1	6.40	0.81	1.38	0.20	1.03	3.08	0.10	8.4	331	576	98	131	28	4	0.738594	20	-18.2	0.6
20120726F(HCl)		42.7	19.2	6.79	0.83	1.49	0.04	0.89	3.28	0.13	10.1	318	554	110	142	31	5	0.737735	14	-18.0	0.4
20120729D(HCl)		46.3	21.4	6.75	0.85	1.61	0.03	0.89	3.76	0.10	10.9	383	675	100	166	32	5	0.750142	30	-21.2	0.2

[1] Suspended sediment concentration

[2] SiO$_2$ concentrations calculated assuming 100% recovery. For a comparison of XRF and ICP-OES concentrations see Table A1

[3] Samples names are YYYYMMDD and the subsequent letters are D=Dryadbreen (glaciated), F= Fardalen (unglaciated) and SG = supraglacial

[4] n=3

Table 2. Relative proportions of clay minerals as determined from XRD patterns for the solid samples collected in the two catchments. Samples are ordered from highest to lowest relative illite abundance.

Sample	Description	Catchment[1]	Illite (%)	I/S (%)	Kaolinite (%)	Chlorite (%)
I[*]	fossil-rich rock	Dr	82	0	9	9
D	sediment (surface of glacier)	Dr	72	12	7	9
R03[*]	litharenite	Dr	67	14	8	10
R04[*]	shale (rock)	Dr	59	26	7	7
A	sandur sediment	Dr	52	28	8	12
F	moraine sediment	Dr	55	28	8	9
O	stream sediment	Dr	51	32	8	9
R02[*]	wacke	Dr	48	33	5	14
H	soil	F	49	35	9	7
M	stream bank sediment	F	51	37	6	7
C	moraine sediment	Dr	44	37	9	10
E[*]	shale rock	Dr	43	40	8	9
R01[*]	shale (pieces)	F	46	40	7	7
N	stream bedload	F	46	41	6	7
L	stream sediment	F	46	43	5	6
K	stream sediment	F	45	43	6	6
B[*]	shale (pieces)	Dr	38	49	6	7
G[*]	shale (pieces)	F	36	50	7	7

[*] Sedimentary (often frost-shattered) rock. All other samples are modern sediments.

[1] Catchment where sample was collected. F=Fardalen, Dr= Dryadbreen.

[2] I/S is an illite-smectite mixed phase mineral.

Appendix A

Table A1. Comparison of element concentrations collected by XRF (only available for four samples) and ICP-OES. Data from ICP-OES is used in the paper.

Name and description	SiO$_2$[1] wt%	Al$_2$O$_3$ wt%	Fe$_2$O$_3$ wt%	TiO$_2$ wt%	MgO wt%	CaO wt%	Na$_2$O wt%	K$_2$O wt%	P$_2$O$_5$ wt%	LOI wt%	Sum wt%	Mn mg/kg	Ba mg/kg	Sr mg/kg	Rb mg/kg	Nd mg/kg	Sm mg/kg
Data collected by XRF																	
R01	63.2	16.3	7.1	0.8	1.4	0.3	1.0	2.6	0.3	7.5	100.5	488	403	97.4	102	35	<10
R02	65.4	13.0	7.9	0.6	1.5	0.6	0.7	2.2	0.3	7.2	99.4	1038	357	81.9	88.8	27	<10
R03	70.9	8.9	3.2	0.6	0.9	6.2	1.1	1.6	0.1	7.0	100.5	472	356	142	55.1	23	<10
R04	57.1	19.1	3.5	0.9	1.3	0.2	0.6	3.6	0.1	12.9	99.3	178	511	116	150	42	<10
Data collected by ICP-OES[1]																	
R01	63.2	15.7	7.1	0.8	1.4	0.4	1.1	2.4	0.2	7.9	100.0	497	438	98	103	32	6
R02	64.7	12.6	8.0	0.6	1.4	0.6	0.8	2.1	0.3	8.9	100.0	1056	371	83	89	26	5
R03	70.0	8.6	3.3	0.6	0.9	6.1	1.1	1.5	0.1	7.7	100.0	480	366	139	54	25	5
R04	58.3	18.5	3.5	0.9	1.3	0.2	0.7	3.2	0.1	13.3	100.0	190	542	107	147	39	7

[1] SiO$_2$ concentrations calculated by assuming 100% recovery.

Table A2. Rare earth element concentrations in mg/kg[1].

Sample[2]	La	Ce	Pr	Nd	Sm	Eu	Gd	Tb	Dy	Ho	Er	Tm	Yb	Lu
Sedimentary rock samples														
R01	35.7	71.2	8.4	32.4	6.0	1.2	4.5	0.7	4.0	0.7	2.0	0.3	1.9	0.3
G	35.7	70.4	8.3	32.3	6.0	1.3	4.6	0.7	4.2	0.8	2.3	0.3	2.2	0.3
R04	49.1	95.4	10.7	39.3	6.6	1.3	4.0	0.7	3.5	0.7	1.9	0.3	1.8	0.2
R02	28.5	55.5	6.6	25.7	4.8	1.1	3.8	0.6	3.2	0.6	1.7	0.2	1.5	0.2
R03	30.5	60.3	6.8	25.4	4.5	0.9	3.1	0.4	2.2	0.4	1.0	0.1	0.9	0.1
Sediment sample														
D	43.9	88.5	9.9	36.5	6.5	1.2	4.3	0.6	3.3	0.6	1.6	0.2	1.4	0.2
Stream sediment samples														
L	37.1	72.8	8.3	31.6	5.8	1.2	4.4	0.7	4.0	0.8	2.2	0.3	2.0	0.3
O	37.9	76.3	8.7	33.4	5.9	1.1	4.2	0.6	3.1	0.5	1.4	0.2	1.3	0.2
<2 μm fraction of bulk rock and sediment samples														
R01-clay	37.0	72.7	9.4	38.1	8.0	1.8	7.1	1.0	5.8	1.0	2.8	0.4	2.5	0.3
R04-clay	38.9	78.0	8.6	31.9	5.8	1.0	3.7	0.6	3.5	0.7	2.0	0.3	2.0	0.3
G-clay	32.4	64.3	8.0	32.6	6.5	1.5	5.7	0.9	4.8	0.9	2.4	0.3	2.2	0.3
D-clay	31.5	64.0	7.0	25.9	4.8	1.0	3.8	0.6	3.4	0.7	1.8	0.3	1.7	0.2
L-clay	30.5	60.4	7.1	29.0	6.0	1.4	5.4	0.9	4.9	1.0	2.7	0.4	2.5	0.4
Suspended sediments (Bulk)[2]														
20120801SG	41.8	82.8	9.4	34.4	6.2	1.2	4.2	0.6	3.3	0.6	1.6	0.2	1.5	0.2
20120617D	40.3	79.3	9.1	34.1	6.2	1.2	4.3	0.6	3.5	0.6	1.6	0.2	1.5	0.2
20120618F	40.9	84.5	10.0	40.3	8.2	1.8	7.1	1.0	5.4	1.0	2.5	0.3	2.0	0.3
20120726F	44.3	89.6	10.4	41.8	8.6	1.9	7.7	1.2	6.3	1.1	2.9	0.4	2.4	0.3
20120729D	44.6	88.9	9.9	37.3	6.6	1.3	4.7	0.7	3.7	0.7	1.8	0.3	1.7	0.3
Suspended sediments (Acid-treated)														
20120617D(HCl)	38.1	72.8	7.9	28.6	4.5	0.7	2.3	0.4	2.2	0.4	1.3	0.2	1.3	0.2
20120618F(HCl)	36.8	71.0	7.8	27.8	4.2	0.9	2.5	0.4	2.7	0.5	1.5	0.2	1.7	0.2
20120726F(HCl)	42.2	81.2	8.8	30.7	4.7	0.9	2.7	0.5	3.0	0.6	1.7	0.3	1.8	0.2
20120729D(HCl)	42.1	80.4	8.8	31.7	4.7	0.9	2.5	0.4	2.4	0.5	1.4	0.2	1.4	0.2

[1] The hotplate digestion method used does not digest zircons and therefore the high rare earth element (HREE) concentrations may be lower than the true total. Nd and Sm are fully digested by the hotplate method (Rickli et al., 2013).

[2] Please refer to Table 1 for sample descriptions.

Table A3. Measurements of four USGS standards by ICP-OES compared to certificate values.

Standard	SiO_2 wt%	Al_2O_3 wt%	Fe_2O_3 wt%	TiO_2 wt%	MgO wt%	CaO wt%	Na_2O wt%	K_2O wt%	P_2O_5 wt%	LOI wt%
SGR-1b										
Mean (n=8)	30.7[1]	6.3	3.3	0.3	4.4	8.1	3.1	1.6	0.1	42.2
2SD		0.4	0.2	0.0	0.3	0.3	0.1	0.1	0.0	0.5
Ref. value	28.2	6.5	3.0	0.3	4.4	8.4	3.0	1.7	0.3	
G-2										
Mean (n=2)	69.0[1]	14.9	3.0	0.6	0.7	2.0	4.2	4.2	0.1	1.4
2SD		0.3	0.0	0.0	0.0	0.0	0.1	0.1	0.0	0.7
Ref. value	69.1	15.4	2.7	0.5	0.8	2.0	4.1	4.5	0.1	
BCR-2										
Mean (n=4)	51.5[1]	13.1	16.5	2.6	3.5	7.0	3.3	1.9	0.1	0.5
2SD		0.3	1.1	0.1	0.1	0.1	0.1	0.1	0.1	0.0
Ref. value	54.1	13.5	13.8	2.3	3.6	7.1	3.2	1.8	0.4	
AGV-2										
Mean (n=2)	58.5[1]	16.4	7.6	1.2	1.7	5.2	4.3	2.9	0.2	2.1
2SD		0.4	0.2	0.1	0.0	0.4	0.2	0.2	0.1	
Ref. value	59.3	16.9	6.7	1.1	1.8	5.2	4.2	2.9	0.5	

[1] SiO_2 concentrations calculated assuming 100% recovery.

For a comparison of XRF and ICP-OES concentrations see Table A1

Table A4. Measurements of four USGS standards by ICP-MS compared to literature value. Concentrations are in mg/kg[1].

Standard	Mn	Rb	Sr	Ba	La	Ce	Pr	Nd	Sm	Eu	Gd	Tb	Dy	Ho	Er	Tm	Yb	Lu
Sco-1																		
Mean (n=12)	431	115	160	627	30.2	59	7.0	27	5.2	1.07	4.2	0.6	3.5	0.69	1.9	0.28	1.79	0.26
2SD	69	19	20	72	4.4	7	0.5	1	0.2	0.08	0.2	0.0	0.2	0.06	0.1	0.03	0.14	0.03
Govindaraju (1994)	410	112	174	570	29.5	62	6.6	26	5.3	1.19	4.6	0.7	4.2	0.97	2.5	0.42	2.27	0.34
BIR-1																		
Mean (n=6)	1419	0.22	105	7	0.69	1.89	0.36	2.4	1.1	0.54	1.98	0.37	2.6	0.58	1.7	0.26	1.72	0.26
2SD	155	0.09	10	1	0.09	0.19	0.02	0.0	0.0	0.04	0.05	0.01	0.2	0.03	0.1	0.01	0.09	0.02
Govindaraju (1994)	1324	0.25	108	7	0.62	1.95	0.38	2.5	1.1	0.54	1.85	0.36	2.5	0.57	1.7	0.26	1.65	0.26
BHVO-2																		
Mean (n=7)	1358	9.59	372	133	15.1	37.0	5.16	24.1	6.05	2.09	6.41	0.95	5.34	0.99	2.56	0.34	2.05	0.28
2SD	89	0.98	35	14	1.7	4.0	0.39	1.2	0.26	0.06	0.22	0.03	0.24	0.04	0.09	0.01	0.09	0.01
Raczek et al. (2001)	1317	9.08	396	131	15.2	37.5	5.29	24.5	6.07	2.07	6.24	0.94	5.32	0.97	2.54	0.34	2.00	0.27
BCR-2																		
Mean (n=9)	1523	47.3	312	657	23.7	50.2	6.39	27.4	6.34	1.88	6.62	1.04	6.29	1.27	3.61	0.53	3.37	0.50
2SD	142	5.8	31	44	2.3	4.1	0.38	0.8	0.14	0.05	0.08	0.02	0.22	0.04	0.15	0.02	0.14	0.02
Raczek et al. (2001)	1471	46.9	340	677	24.9	52.9	6.57	28.7	6.57	1.96	6.75	1.07	6.42	1.30	3.66	0.56	3.38	0.52
AGV-2																		
Mean (n=6)	785	70.3	616	1141	37.7	68.3	7.94	30.2	5.48	1.43	4.29	0.64	3.49	0.67	1.85	0.27	1.68	0.25
2SD	75	8.2	45	121	4.1	6.8	0.54	1.4	0.22	0.05	0.23	0.01	0.15	0.04	0.10	0.01	0.08	0.01
Raczek et al. (2001)	774	66.3	661	1130	37.9	68.6	7.68	30.5	5.49	1.53	4.52	0.64	3.47	0.65	1.81	0.26	1.62	0.25

[1]The hotplate digestion method used does not digest zircons and this accounts for the low recovery of the HREE in the sedimentary standard SCo-1.